AD-A106 415 BEDFORD RESEARCH ASSOCIATES MA F/G 4/1
DETERMINATION OF IONOSPHERE CRITICAL FREQUENCY FOF2,(U)
JUN 80 R BOUCHER, J P NOONAN F19628-79-C-0163
UNCLASSIFIED SCIENTIFIC-2 AFGL-TR-80-0346 NL

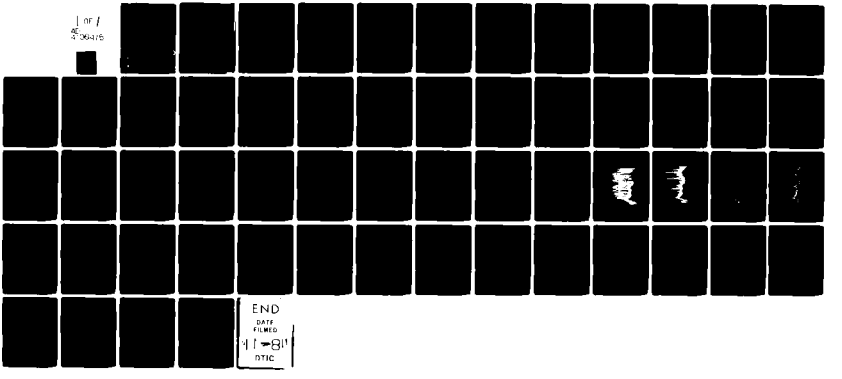

END
DATE FILMED
11-81
DTIC

LEVEL II

(2)

(19)

(18) AFGL-TR-80-0346

(6) DETERMINATION OF IONOSPHERE CRITICAL FREQUENCY f_0F2

(10) R. Boucher
J.P. Noonan

Bedford Research Associates
2 DeAngelo Drive
Bedford, Massachusetts 01730

(14) Scientific [redacted]-2

(11) 30 Jun [redacted]80 (12) 56

(15) F19628-79-C-0163 (16) 9993 (17) XX

Approved for public release; distribution unlimited

AIR FORCE GEOPHYSICS LABORATORY
AIR FORCE SYSTEMS COMMAND
UNITED STATES AIR FORCE
HANSCOM AFB, MASSACHUSETTS 01731

SECURITY CLASSIFICATION OF THIS PAGE (When Data Entered)

REPORT DOCUMENTATION PAGE		READ INSTRUCTIONS BEFORE COMPLETING FORM
1. REPORT NUMBER AFGL-TR-80-0346	2. GOVT ACCESSION NO. AD-A106415	3. RECIPIENT'S CATALOG NUMBER
4. TITLE (and Subtitle) DETERMINATION OF IONOSPHERE CRITICAL FREQUENCY f_0F2		5. TYPE OF REPORT & PERIOD COVERED Scientific Report No. 2 6. PERFORMING ORG. REPORT NUMBER
7. AUTHOR(s) R. Boucher J.P. Noonan		8. CONTRACT OR GRANT NUMBER(s) F19628-79-C-0163
9. PERFORMING ORGANIZATION NAME AND ADDRESS Bedford Research Associates 2 DeAngelo Drive Bedford, MA. 01730		10. PROGRAM ELEMENT, PROJECT, TASK AREA & WORK UNIT NUMBERS 62101F 9993XXXX
11. CONTROLLING OFFICE NAME AND ADDRESS Air Force Geophysics Laboratories Hanscom AFB, MA. 01731 Monitor/P.Tsipouras/SUWA		12. REPORT DATE 30 June 1980 13. NUMBER OF PAGES 57
14. MONITORING AGENCY NAME & ADDRESS(if different from Controlling Office)		15. SECURITY CLASS. (of this report) UNCLASSIFIED 15a. DECLASSIFICATION/DOWNGRADING SCHEDULE

16. DISTRIBUTION STATEMENT (of this Report)

Approved for public release; distribution unlimited

17. DISTRIBUTION STATEMENT (of the abstract entered in Block 20, if different from Report)

18. SUPPLEMENTARY NOTES

19. KEY WORDS (Continue on reverse side if necessary and identify by block number)

f_0F2, Ionospheric F2 Layer, Critical frequency estimation.

20. ABSTRACT (Continue on reverse side if necessary and identify by block number)

This report describes an estimation procedure for determining the critical frequency of the ionospheric F2 layer. The estimate is obtained from measurements of radio noise obtained by a satellite orbiting above the F2 layer. A spectrum analyzer obtains noise power as a function of frequency in a band wide enough to include all possible values of the critical frequency.

DD FORM 1 JAN 73 1473

UNCLASSIFIED

SECURITY CLASSIFICATION OF THIS PAGE (When Data Entered)

INTRODUCTION

Defense Meteorological Satellite is equipped with a swept-frequency HF noise receiver. The receiver provides measurements of radio noise of terrestial origin every 100 KHz in the frequency range of 1.2 to 13.9 Mhz. Satellite is basically in a sun-synchronous morning or evening orbit. By analyzing data from successive morning or evening orbit, global maps of the noise intensity can be obtained at the satellite altitude. Work is being done in order to obtain world maps of noise intensity so as to assess the morphological behavior of the noise at satellite altitude as a function of frequency. Our studies have been concentrated on the frequencies of 1.5 to 13.5 Mhz in steps of 0.5 Mhz at both the dawn and dusk orbits. Monthly average noise maps are obtained in order to provide more representative maps of the average noise behavior.

The Air Force Global Weather Central processes several types of special sensor data including the data from the swept-frequency HF noise receiver. The DMSP tapes have been processed by GWC on the UNIVAC 1110 system, where the word length is 36 bits.

We next present a description of the overall software used in this study. Following this is a report deriving the optimal procedure for estimating the FoF2 of the Ionosphere.

IONOSPHERIC RADIO NOISE MEASUREMENT

SOFTWARE

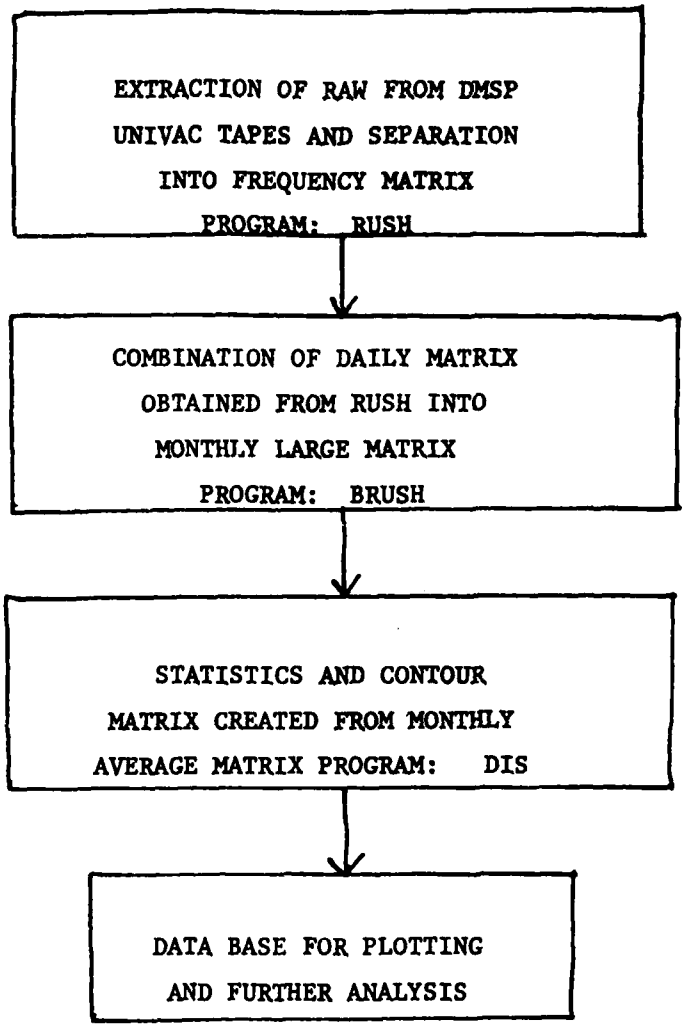

SOFTWARE DESCRIPTION

PROGRAM: RUSH

RUSH unpacks data from one DMSP satellite tape. UNIVAC record is read and put into CDC words. All frequencies between 1.5 and 13.5 Mhz in steps of 0.5 Mhz are translated and loaded into frequency, latitude, and longitude matrix.

PROGRAM: BRUSH

Intermediate step before statistical analysis. Data files created by RUSH are combined until monthly matrix is complete. Up to five data sets will be combined with an existing data file.

PROGRAM: DIS

Program displays average count matrix for dawn and dusk and statistics about these matrices. Also printer contour is done to provide high and low noise peak for each frequency, at each latitude and longitude.

Data Base generated now used for further analysis such as estimates foF2 as described in this report.

I INTRODUCTION

This report describes an estimation procedure for determining the critical frequency of the ionospheric F2 layer. The estimate is obtained from measurements of radio noise obtained by a satellite orbiting above the F2 layer. A spectrum analyzer obtains noise power as a function of frequency in a band wide enough to include all possible values of the critical frequency.

The power measured at a particular frequency is a function of the radio energy being transmitted, and the transmittance of the F2 layer. The ionospheric parameters depend on the position of the satellite (particularly latitude), local time, and solar activity. The noise measured by the satellite receiver is considered to consist of two parts. The first is referred to as terrestrial noise, which passes through the F2 layer. This noise originates from such sources as radio transmitters located near the subsatellite point. The other component is background noise, which is not affected by the F2 layer, and can originate from within the satellite instrumentation itself or other sources located above the F2 layer.

The available data comes from a DMSP satellite with an on-board swept-frequency receiver. Counts are obtained for 128 frequency channels from 1.2 MHz to 13.9 MHz in increments of 100 KHz. One important aspect of the data is that there is coupling between adjacent channels, that is, a fraction of the power at one particular channel is also picked up by adjacent channels. This is most likely caused by the bandwidth of each channel filter being wider than the interchannel separation. While this produces some smoothing of the data, it also modifies the probability distribution of the data from what one would normally expect. Thus, it must be dealt with before the model of the data is constructed.

For estimation of the critical frequency foF2, the maximum likelihood (ML) technique is the method of choice. It is a well known and studied estimation method. For most applications it is well behaved and the optimum method. It is also systematic and intuitively meaningful since it can be derived directly from the model of the data.

II THEORY OF ESTIMATION METHOD

A. The Model

The effect of the foF2 layer on the radio noise spectrum received by the satellite can be modelled as a high pass filter. There are many candidate filters which can be used. For our purposes, it is desirable to use a filter with the least number of parameters, since each parameter must either be estimated or assigned a value. A suitable filter is the Butterworth filter of order n.

$$\left| H_n(f) \right|^2 = \frac{1}{1 + \left(\frac{fo}{f}\right)^{2n}} \qquad (1)$$

The parameter fo thus becomes the ionospheric critical frequency. The filter order n must also be chosen. Our procedure will be to choose several values for n and observe its effect on the estimation procedure.

The satellite receiver measures the power at discrete frequencies. A record of count data can be expressed as

$$S(f_k) = S_N(f_k) + \left| H_n(f_k) \right|^2 S_T(f_k) \qquad (2)$$
$$\text{for } k = 1,\ldots,N$$

where $S_N(f_k)$ is the noise power due to background and instrumentation noise, and $S_T(f_k)$ is the noise power due to radio signals of terrestrial origin which are affected by the F2 layer. However, S_N and S_T are random processes whose moments are unknown functions of frequency. In the absence of such information about these signals, we need to make certain assumptions;

namely, that these moments are constant with respect to frequency. In actuality, we need only consider one of the moments (such as the mean or variance) since these signals are chi-square distributed with all moments dependent on one of the moments. Thus, we obtain one additional parameter for S_N and one for S_T which must be estimated, along with the important quantity fo.

The problem can thus be expressed as a classical parameter estimation problem. The procedure is as follows:

1. Preprocess the data into a form acceptable by the estimation method, described in part B.
2. Estimate the critical frequency fo (and the S_N and S_T parameters as a by-product) by the maximum likelihood method (ML), described in part C.

Also in this chapter, part D describes and derives the Cramer-Rao bound for the estimated fo. Part E extends the method to include an arbitrary signal noise power function. Part F discusses a method for obtaining initial estimates of the S_N and S_T parameters which can then be used in the estimation procedure of part C.

B. Preprocessing of the Data

In the absence of interchannel coupling, each frequency channel would be a chi-square distributed random variable with two degrees of freedom. However, since each filter in the bank of filters has a finite, but unknown, bandwidth larger than the separation between channels, the received record is then expressed as the original power spectrum convolved with some "smearing function". Consequently, the degrees of freedom of each channel is increased.

The estimation method requires that the distribution of the data be of known form. Furthermore, computational efficiency is gained if the

channels are uncorrelated among themselves. The solution is to remove the effect of coupling by filtering the record in the frequency domain by a digital filter:

$$X(f_k) = \sum_{m=-M}^{M} S(f_{k-m})\, h_d(m) \qquad k=1,2,\ldots,N$$

$X(f_k)$ is a nearly-Gaussian, zero mean, uncorrelated (and therefore independent) process. The filter $h_d(m)$ is a nonrecursive zero-phase (symmetric) digital filter, designed by the McClellan-Parks algorithm [1], of length $2M+1 = 41$ with an attenuation of 40 dB in the stopband. The problem encountered at the edges of the record is dealt with by extending the record at each end by its mirror image

$$S\left(f_{1-n}\right) = S\left(f_{1+n}\right) \text{ and } S\left(f_{N+n}\right) = S\left(f_{N-n}\right)$$

for $n = 1,\ldots,M$ and $N = 128$.

This processed record can then be expressed as

$$X(f_k) = N(f_k) + \left| H_n(f_k) \right|^2 T(f_k) \qquad (3)$$

where $N(f_k)$ and $T(f_k)$ are independent Gaussian variables, with zero mean, but a variance which depends on the signal strength S_N and T_N. The variance of $X(f_k)$ is

$$\sigma_x^2(f_k) = \sigma_N^2 + \left| H_n(f_k) \right|^4 \sigma_T^2 \qquad (4)$$

C. Maximum Likelihood Estimation

Parameter estimation via the maximum likelihood technique can be expressed intuitively as follows. We have a model, with parameters that can be chosen. Given an observation $\underline{X}$, what choice of parameters make the given observation most likely to have happened? In the context of the above model, the parameter vector is

$$\underline{\Theta} = [\, f_o, \sigma_N^2, \sigma_T^2 \,]$$

and the observation vector is the preprocessed record

$$\underline{X} = [X(f_1), X(f_2), \ldots, X(f_N)] = [x_1, x_2, \ldots, x_N].$$

The (ML) estimation procedure involves finding the probability density of $\underline{X}$ as a function of the parameter vector $\underline{\Theta}$, $p(\underline{X};\underline{\Theta})$ which is then maximized with respect to $\underline{\Theta}$. In practice, the likelihood function $l(\underline{\Theta})$ is maximized, where

$$l(\underline{\Theta}) = \log p(\underline{X};\underline{\Theta}).$$

After preprocessing, the channels are independent zero-mean Gaussian variables. The probability density can be expressed simply as

$$p\,(\underline{X};\, f_o, \sigma_N^2, \sigma_T^2) = \prod_{k=1}^{N} \frac{1}{\sqrt{2\pi}\,\sigma_x(f_k)} \exp\left[-\frac{1}{2} \frac{X_k^2}{\sigma_x^2(f_k)} \right] \quad (5)$$

where σ_x^2 is obtained from (4).

The likelihood function is

$$l\,(f_o,\ \sigma_N^2,\sigma_T^2) \;=\; -\frac{N}{2}\log 2\pi - \frac{1}{2}\sum_{k=1}^{N}\left[\log \sigma_x^2(f_k) + \frac{X_k^2}{\sigma_x^2(f_k)}\right] \qquad (6)$$

The first term can be ignored since it does not depend on the parameters. The ML estimate is obtained from

$$\text{maximize } l(\underline{\theta}) = -\sum_{k=1}^{N}\left[\log \sigma_x^2(f_k) + \frac{X_k^2}{\sigma_x^2(f_k)}\right] \qquad (7)$$

$$\text{where } \sigma_x^2(f_k) = \sigma_N^2 + \left[\frac{1}{1+\left(\frac{f_o}{f_k}\right)2n}\right]^2 + \sigma_T^2$$

We can try to locate the maximum by taking the partial derivatives with respect to f_o, σ_N^2, σ_T^2 and eauate to zero. However, this yields a complex set of coupled nonlinear equations, and the solution of these equations does not guarantee a global maximum.

Instead, the solution is found numerically. This is a three-dimensional maximization, and some gradient directed algorithm would seem to be called for. However, $l(\underline{\theta})$ is itself a random process, making its gradient too unreliable for such a sensitive algorithm. Instead, the following iterative approach is used:

1. Obtain initial estimates for σ_N^2 and σ_T^2. These can be rough guesses, or they can be obtained by the method in part F.

2. Keeping σ_N^2 and σ_T^2 constant, maximize l by a one-dimensional Fibonacci search on f_o.

3. Keeping σ_N^2 and f_o constant, do Fibonacci search on σ_T^2.
4. Keeping σ_T^2 and f_o constant, search for σ_N^2.
5. Go back to step 2 and repeat until convergence is achieved.

This method has been shown to be reliable with the given data, and converges in about three or four iterations, when initial estimates of σ_N^2 and σ_T^2 are provided by the method of part F.

D. Cramer-Rao Bound

Since the estimated f_o is a random variable, it would be useful to determine its mean and variance, and hence determine the accuracy of the estimator. For most nonlinear estimation problems, this is a difficult task. However, the theory does provide a quantity known as the Cramer-Rao bound, which is a lower bound on the variance of the estimate. This bound depends only on the model and the statistics of the data, and is independent of the actual estimation technique used. While it is not as useful as an upper bound, it is an inherent property of the data itself, and can tell us if our expectations concerning estimation accuracy are reasonable.

There are two formulas for calculating this bound [2]. In this case, the easier one is

$$\text{Var}[f_o] \qquad \text{CRB} = \left[-E \left(\frac{\delta^2 \log p\left(\underline{X}; f_o\right)}{\delta f_o^2} \right) \right]^{-1} \tag{8}$$

We are interested only in the parameter f_o. Suppose σ_N^2 and σ_T^2 are constants. The likelihood function is

$$l(f_o) = \log p(\underline{X}\ ;\ f_o,\ \sigma_N^2,\ \sigma_T^2) = -\frac{N}{2} \log 2\pi - \frac{1}{2} \sum_{k=1}^{N} \left[\log \sigma_x^2(f_k) + \frac{X_k}{\sigma_x^2} \right]$$

where

$$\sigma_x^{\,2}(f_k) = \sigma_N^{\,2} + g_n^{\,2}(f_k)\,\sigma_T^{\,2}$$

and define

$$g_n(f_k) = \left| H_n(f_k) \right|^2 = \frac{1}{1 + \left(\frac{f_o}{f_k}\right)^{2n}}$$

Then

$$\frac{1(f_o)}{f_o} = -\frac{1}{2} \sum_{k=1}^{N} \left(\frac{1}{\sigma_x^{\,2}(f_k)} - \frac{X_k^{\,2}}{\sigma_x^{\,4}(f_k)} \right) \sigma_T^{\,2} \; \frac{-4n f_o^{\,2n-1}}{f_k^{\,2n}} \; g_n^{\,3}(f_k)$$

$$\frac{2\,1(f_o)}{f_o} = -\sum_{k=1}^{N} \left\{ \left(\frac{2X_k^{\,2}}{\sigma_x^{\,2}(f_k)} - 1 \right) \frac{\sigma_T^{\,4}}{\sigma_x^{\,4}(f_k)} \; \frac{8n^2 f_o^{\,4n-2}}{f_k^{\,4n}} \; g_n^{\,6}(f_k) \right.$$

$$\left. + \left(1 - \frac{X_k^{\,2}}{\sigma_x^{\,2}(f_k)} \right) \frac{\sigma_T^{\,2}}{\sigma_x^{\,2}(f_k)} \; \frac{2n\, f_o^{\,2n-2}}{f_k^{\,2n}} \; g_n^{\,3}(f_k) \; \frac{6\, f_o^{\,2n}}{f_k^{\,2n}} - 2n + 1 \right] \right\}$$

Taking the expectation over X, $E[X_k^{\,2}] = \sigma_x^{\,2}(f_k)$ results in

$$-E\left[\frac{2_1(f_o)}{f_o^{\,2}} \right] = \sum_{k=1}^{N} \frac{\sigma_T^{\,4}}{\sigma_x^{\,4}(f_k)} \; \frac{8n^2 f_o^{\,4n-2}}{f_k^{\,4n}} \; g_n^{\,6}(f_k)$$

and the bound is

$$CRB = \left[8n^2 \sum_{k=1}^{N} \frac{\sigma_T^{\,4}}{\sigma_x^{\,4}(f_k)} \; \frac{f_o^{\,4n-2}}{} \; g_n^{\,6}(f_k) \right]^{-1} \qquad (9)$$

The bound depends on the parameters f_o, σ_N^2, σ_T^2 as well as on the filter order n. Sufficient accuracy can be obtained by using the estimated values of the parameters instead of the true values. Generally, the bound is lower for higher values of filter order n. It also decreases as σ_N^2 (background noise power) decreases.

Although there is no guarantee that an estimator meets the Cramer-Rao bound, some good properties of the ML estimator recommend its use. The ML estimator is consistent, i.e., as N (the number of observations) increases. the estimate converges to the true value. The ML estimator is also asymptotically efficient, i.e., as N increases, the variance tends toward the Cramer-Rao bound. Thus, the performance of a ML estimator can be improved by sampling the frequency spectrum more finely.

E. Extension to Arbitrary $S_T(f)$

In the previous sections, we assume that the variance of T(f) is constant over frequency. This assumption can be relaxed if information about the transmitted terrestrial radio noise is available. Then equation (3) can be modified as

$$X(f_k) = N(f_k) + \left| H_n(f_k) \right|^2 T_o(f_k) R(f_k)$$

where the variance of T_o dos not depend on frequency. $R(f_k)$ is a function which expresses the relative terrestrial noise power in the frequency band. It can be multiplied by any scale factor as convenient. The variance of X becomes

$$\sigma_x^2(f_k) = \sigma_n^2 + \left| H_n(f_k) \right|^2 R^2(f_k) \sigma_T^2 \qquad (10)$$

which can then be used in the maximum likelihood formulation of equation (7).

The Cramer-Rao bound becomes

$$CRB = 8_n^2 \sum_{k=1}^{N} \left[\frac{\sigma_T^4}{\sigma_X^4 (f_k)} \quad \frac{f_o^{4n-2}}{f_k^{4n}} R^4 (f_k) g_n^6 (f_k) \right]^{-1} \qquad (11)$$

Thus if the signal power being transmitted near the subsatellite point is known, it can be included in the above technique. In the absence of such information, the assumption $R(f_k)$ = constant must be made.

F. Initial Estimates of σN^2 and σT^2

Estimates of σ_N^2 and σ_T^2 are obtained by another maximum likelihood technique used in supervised learning [3]. Suppose the ionosphere behaves as an ideal filter. Then there are two cases

W1: Case 1. $S_N(f)$ only present $\sigma_X^2 = \sigma_N^2 = \sigma_1^2$

W2: Case 2. $S_N(f)$ and $S_T(f)$ present $\sigma_X^2 = \sigma_N^2 + \sigma_T^2 = 2^2$

The probability density of X_k can be described as the following mixture density

$$p(X_k;\underline{\theta}) = \sum_{j=1}^{2} p(X_k \mid W_j; \sigma_j^2) \; P(Wj) \qquad (12)$$

where $P(W_1)$ is the proportion of channels for which Case 1 applies, and $P(W_2)$ the proportion for which Case 2 applies, with $P(W_1) + P(W_2) = 1$, and the parameter vector is $\underline{\theta}$ is (σ_1^2 , σ_2^2). The log likelihood function is

$$1\ (\underline{\theta}) = \sum_{k=1}^{N} \log p(X_k;\underline{\theta}) \qquad (13)$$

the derivative with respect to σ_1^2 is

$$\frac{\partial l}{\partial \sigma_i^2} = \sum_{k=1}^{N} \frac{1}{p(X_k;\underline{\theta})} \frac{\partial}{\partial \sigma_i^2} [p(X_k \; W_i \; ; \sigma_i^2) \; P(w_i)$$

Noting that $P(W_1 \; X_k \; ; \sigma_i^2) = \dfrac{p \; (X_k \; W_i \; , \; \sigma_i^2) \; P(W_i)}{p \; (X_k \; ; \underline{\theta})}$

we can obtain the useful form

$$\frac{\partial l}{\partial \sigma_i^2} = \sum_{k=1}^{N} P(W_i / X_k \; ; \; _k{}^2) \frac{\partial}{\partial \sigma_i^2} \log p(X_k / W_i \; ; \sigma_i^2) = 0 \qquad (14)$$

Now since X_k is Gaussian and zero mean,

$$\log p(X_k \; W_i \; ; \; \sigma_i^2) = -\frac{1}{2} \log 2\pi - \frac{1}{2} \log \sigma_i^2 - \frac{1}{2} \frac{X_k^2}{\sigma_i^2}$$

and then

$$\frac{\partial l}{\partial \sigma_i^2} = -\frac{1}{2} \sum_{k=1}^{N} P \; (W_i / X_k \; ; \sigma_i^2) \; (1 - \frac{X_k^2}{i^2}) \; \frac{1}{\sigma_i^2} = 0 \qquad (15)$$

The above cannot be solved in closed form, but an iterative approach can be used:

$$\sigma_i^2 \; (\text{new}) = \frac{\sum_{k=1}^{N} P \; (W_i \; / X_k \; ; \sigma_i^2) \; X_k^2}{\sum_{k=1}^{N} P \; (W_i / X_k \; ; \sigma_i^2)} \qquad (16)$$

where

$$P \; (W_i / X_k \; ; \sigma_i^2) = \frac{P \; (X_k / W_i \; ; \sigma_i^2) \; P \; (W_i)}{\sum_{j=1}^{2} P \; (X_k / W_j \; ; \sigma_j^2) \; P \; (W_j)} \qquad (17)$$

The $P(W_i)$ are also unknown. They are also found iteratively by

$$P(W_i)^{(new)} = \frac{1}{N} \sum_{K=1}^{N} P(W_i / X_k ; \sigma_i^2) \qquad (18)$$

Equations (16-18) provide the method used to obtain initial estimates of the σ_i^2, and therefore σ_N^2. Typically this algorithm is run for about ten iterations, and the results then used in the estimation method of Part C.

REFERENCES

[1] J. H. McClellan, T. W. Parks, L. R. Rabiner "A Computer Program for Designing FIR Linear Phase Digital Filters" IEEE Trans. on Audio and Electroacoustics, Vol AU-21, No. 6, 506-526 - December 1973.

[2] H. L. Van Trees Detection, Estimation and Modulation Theory, Part 1. John Wiley and Sons, Inc., New York, 1968 Chapter 2.4.2

[3] R. O. Duda, P. E. Hart Pattern Classification and Scene Analysis John Wiley & Sons, Inc., New York 1973 pp 192-201

III - RESULTS

A - Data Description

Data was extracted from the tapes for the month of December, 1977, and for two global locations. The first was a strip 5^{o} wide centered at 37.3^{o} E longitude, from 0^{o} to 70^{o} N latitude. This data includes Moscow (55.3^{o} N, 37.3^{o} E). The second set of data is a strip 5^{o} wide centered at 105.3^{o} W longitude, from 0^{o} to 70^{o} N latitude, which includes Boulder (40.0^{o} N, 105.3^{o} W). Data was taken for both sunrise and sunset periods.

Each record in the original data contains the date, time, coordinates, and 240 channels of count data. From this, a record consisting of channels 0-127 inclusive could usually be extracted. When this could not be done, as in the case of missing data, the record was discarded. Channel 0 corresponds to 1.2 MHz, with increments of 100 KHz between channels. Each count is a 7 bit value, ranging from 0 to 127.

Composite plots of the counts for all records from 0^{o} to 70^{o} N are shown in Figure 1a for Moscow and Figure 1b for Boulder. Figure 2 displays the counts within a latitude and longitude window 5^{o} square centered on Moscow (Figure 2a) and Boulder (Figure 2b).

Several observations can be made concerning this data. The expected distribution for this type of data is normally chi-square with two degrees of freedom. However, this is not the case here, since coupling between channels causes some averaging and this raises the degrees of freedom to some unknown number. The amount of averaging depends on the bandwidth of the filters used for each channel, and is unknown. Also present in the data is a distinctive "tail" which is apparently independent of time and global location. This tail is a function of frequency and consists of a spike at 1.2 MHz, a dip at 1.3, a peak at 1.7, a dip at 1.9, and a peak at 3 MHz. It is present in both Moscow and Boulder data, which indicates that it is some type of instrument noise. Since this noise is not stationary, it

must be removed before the estimation of f_0F2 can proceed.

The data was preprocessed by filtering in the frequency domain with a high pass filter. This accomplishes three things. First, the noise tail described above is removed. Also, filtering cancels the effect of coupling between channels, resulting in an uncorrelated process. Furthermore, the additional filtering renders the data more nearly Gaussian by the central moment theorem. The results is a zero mean Gaussian process.

Much of the data is distorted by the limited dynamic range of the receiver. This distortion is especially prominent in the Moscow data, where the strong signal causes clipping at the maximum count value of 127 Figures 1a and 2a). Signal strength for the Boulder data is much less. The signal is buried in the background noise, except for the frequencies which correspond to the shortwave broadcast bands. These peaks also occur in the Moscow data, but they are not visible because of the clipping.

B - Estimation Examples

The estimation procedure will be demonstrated using sample records from the Moscow and Boulder files. Figure 3a shows the original count data for Moscow day 336 (December 2, 1977), ISEC=63845 (17:44 UT or 19:44 local time), latitude 56.64° N, longitude 35.73° E. The result after the filtering is shown in Figure 3b. This data is modeled as in EQ. 3, and is input to the f_0F2 estimation algorithm. Several values of n, the order of the model filter Hn(f), were tried in order to observe its effect on accuracy and convergence of the algorith. The likelihood function (Eq. 7) at the final iteration is plotted in Figures 3c-3g for filter orders n=1 to n=5 respectively. Table 1 contains the estimates of σ_N^2, σ_T^2, f_0 at each iteration for these values of n.

For this data, it can be seen that higher values of n result in better convergence. Higher values of n yield lower estimates of f_0. Agreement with the ionosonde value is better for the higher order filters. An

ideal filter model (with an effective n of infinity) gives a slightly lower value of f_0, but the likelihood function is not very stable. Ionosonde values for December 2 are 3.3 MHz at 19:00 and 1.9 MHz at 20:00, with an interpolated value of 2.3 at 19:44 local time.

Another example is taken from the Boulder data, day 336 (December 2), ISEC=50316 (13:58 UT or 6:58 local time), latitude 42.36° N, longitude 249.51° E (110.51° W). The original count data is shown in Figure 4a, and the data after high pass filtering in Figure 4b. Table 2 contains the estimates of σ_N^2, σ_T^2, and f_0 for each iteration and n=1 to n=5. Figures 4c-4g show the likelihood function at the final iteration for this sequency of n=1 to 5.

In this example, the correct estimate is not achieved. This is caused by the characteristics of the data mentioned previously. A comparison of the Boulder and Moscow examples reveals the difference. In the Boulder data, the signal strength is weak in the region near f_0F2. The spectrum is not stationary, but is dominated by the peaks occuring at the broadcast bands, notably near 6, 10 and 12 MHz. The likelihood functions (Figures 4c-4g) show a peak near 6 MHz. As n increases, resolution increases, and another peak near 4 MHz becomes visible. In the Moscow data, the signal is stronger over the entire spectrum, but the peaks at the broadcast bands are clipped. Consequently, the likelihood function exhibits a dominant peak near the expected f_0F2 frequency.

Note that in both of these examples, the likelihood function has a small peak at 1.2 MHz. This is due to the spike at that frequency in the original data. In some cases, this peak was the largest, resulting in an erroneous estimate. This problem was rectified by modifying the search algorithm so that it ignored this peak.

C - Results On Complete Files

The estimation program was run on both files of data. Estimates were obtained for two strips 5° wide and from 0° N to 70° N described previously.

Tabulated estimates of σ_N^2, σ_T^2 and f_0 are to be found in Table 3 for the Moscow file and Table 4 for the Boulder file. All of these estimates were obtained using a model filter order n=5.

It is informative to plot this data as a function of latitude. Figure 2 shows estimated f_0 versus latitude for the Moscow file. The morning passes are in Figure 5a, and evening passes are in Figure 5b. The inverse relation between f_0F2 and latitude is readily apparent. However, the Boulder estimates (Figures 6a and 6b) do not show this relation. Thus, it is clear that f_0F2 is being correctly estimated for the Moscow data but not for the Boulder data.

Selected records of the data are examined more closely in Tables 5 and 6. Those passes within a 5^o square window over the specified location are included with Moscow in Table 5 and Boulder in Table 6. Columns 5-7 list the estimates of σ_N^2, σ_T^2 and f_0F2. In column 8 is the square root of the Cramer-Rao bound, i.e. the lower bound of the standard deviation of the estimate. Column 9 lists the observed f_0F2 values as obtained from the gound based ionosonde at each station.

A comparison of the estimated and observed values points out the difference between the two files. Define the difference $d=f_0$ (estimated) - f_0 (ionosonde). For the Moscow data, the average of d is 0.66 MHz, and the standard deviation is 0.585 MHz. The average (RMS) of the Cramer-Rao bound values is 0.574 MHz. The estimator appears to have a variance near the Cramer-Rao bound, but there is a bias of 0.66 MHz. The average Cramer-Rao bound in this case is 0.38 MHz. The large average error and large difference between σ^2 and the Cramer-Rao bound indicates the failure of the estimator for this data.

D - Discussion, Conclusions

The way f_0 is defined has some impact on its estimation and the bias when compared to other measurement methods. Here, f_0 is defined in the

usual sense as the half-power (3dB point). When the ionosphere is modelled as a high-pass Butterworth filter, the parameter f_0 conforms to this convention. The width of the transition band is controlled by the parameter n. It has been observed that higher n gives better convergence and lower estimates of f_0. If n is too high, however, the log likelihood function is not smoothed enough, and tends to become irregular and less stable.

The performance of any estimator depends on the information available for its use. When such information is not available, assumptions must be made. When the data does not meet these assumptions, the result is an erroneous estimate. The important properties which will affect any estimator are the distributions of $S_N(f)$ and $S_T(f)$.

Because of the overlap between members of the filter band in the noise receiver, the number of degrees of freedom of the noise is raised to some unknown number. Furthermore, the background noise $S_N(f)$ is non-stationary, since its mean (and possibly its variance) is a function of frequency. Our recourse is to high pass filter the data in the frequency domain.

A deficiency of the receiver is its limited dynamic range and lack of gain control. Consequently, the received signal is either clipped (in the Moscow case) or too small to be measured (in the Boulder case). Also, the signal $S_T(f)$ is nonstationary because of varying shortwave activity. Since this activity is not known a priori, we must assume stationarity and use the method of II C. In the case of the Boulder data, the estimator is often fooled by the peak at the 49 meter broadcast band.

The maximum likelihood method is not the only estimator which would suffer. Heuristic methods can also be fooled by the nonstationarity of the noise. Improvements can be made if the following were available:

- More detailed specifications on the channel filters of the noise receiver. This would allow us to determine the distribution of the data, and reconstruct the original power spectrum.

- Measurements of the background noise $S_N(f)$ mean and variance due to instrumentation.

- Larger dynamic range and better gain control of the receiver.

- Determination of broadcast activity at the ground point beneath the satellite. This would made $R(f_k)$ available, so that the technique of II E could be used.

TABLE I

f_0 convergence for various n, Moscow day 336, ISEC = 63845

n	σ_N^2	σ_T^2	f_0
1	16.5672	133.420	1.3821
	24.8508	116.587	2.5610
	37.2763	127.057	3.8094
	44.9023	138.468	4.7237
2	16.5672	133.420	3.0875
	24.8508	127.119	3.2501
	37.2763	119.837	3.5692
	45.9023	109.076	3.8338
3	16.5672	133.420	3.0305
	24.8508	120.256	3.1017
	37.2763	111.555	3.2896
	44.7342	99.641	3.3627
4	16.5672	133.420	2.9876
	24.8508	117.258	3.0436
	37.2763	108.409	3.1956
	44.2439	96.495	3.2594
5	16.5672	133.420	2.9584
	24.8508	115.503	3.0192
	37.2763	107.008	3.1562
	44.0565	95.042	3.2107

TABLE 2

f_0 convergence for various n, Boulder day 336, ISEC = 50316

n	σ_N^2	σ_T^2	f_0 (MHz)
1	9.7235	118.343	1.2
	14.5852	108.591	1.2
	21.8778	100.605	1.2
	32.4869	89.8603	3.6667
2	9.7235	118.343	4.3515
	14.5852	129.425	4.6541
	21.8778	131.175	4.9546
	32.4869	128.334	5.3827
3	9.7235	118.343	4.3279
	14.5852	120.678	4.4652
	21.8778	117.459	4.7294
	32.4869	112.276	5.4372
4	9.7235	118.343	4.2279
	14.5852	115.867	4.2944
	21.8778	111.114	4.4626
	32.4869	104.536	5.6286
5	9.7235	118.343	4.1584
	14.5852	113.261	4.1944
	21.8778	108.046	4.2769
	32.4869	100.771	5.7168

TABLE 3 - ESTIMATES FOR ENTIRE "MOSCOW" FILE

	TIME	LAT.	LONG(E)	σ_N^2	σ_T^2	f_0F2
335	63645	56.64	35.73	4.40566E+01	9.50423E+01	3.21367E+00
336	63785	60.03	38.04	4.39841E+01	8.62859F+01	3.67246E+00
337	62953	47.12	35.13	4.39033E+01	4.56831E+01	3.01346E+00
337	62923	50.57	36.76	2.73097E+01	5.76107E+01	2.26525E+00
337	62853	54.01	36.52	2.95892E+01	5.26655E+01	2.60132E+00
338	12883	65.86	36.29	4.15537E+01	1.13716F+02	3.18629E+00
338	17159	8.51	35.13	9.04299E+01	1.53290E+02	7.63929E+00
338	17099	2.97	35.95	1.01844E+01	1.91698E+02	7.38758E+00
339	16374	20.85	35.98	1.46047E+01	1.75421E+02	7.70311E+00
339	16314	17.31	36.67	1. 9028E+0	1.99032E+02	7.76117E+00
339	16254	13.77	37.74	8.47049E+00	1.88388E+02	7.74611E+00
339	16194	10.24	38.58	6.68658E+00	1.59658E+02	7.81558E+00
339	16134	6.70	39.41	9.84315E+00	1.35320E+02	7.73104E+00
341	54742	61.15	35.15	4.25720E+01	9.34804E+01	3.68177E+00
341	54662	64.49	35.12	3.27146E+01	1.14040E+02	3.58536E+00
342	13886	55.66	38.39	3.54254E+01	1.13211E+02	3.26873E+00
342	13826	52.22	38.27	3.71889E+01	1.00111E+02	3.29886E+00
343	62908	47.37	35.89	4.90413E+01	5.29233E+01	3.80940E+00
343	62843	50.81	37.45	5.10094E+01	6.09873E+01	8.16430E+00
343	52733	54.24	39.23	4.33198E+01	8.553 1E+01	2.45410E+00
344	11992	64.84	37.96	4.37185E+01	1.22994E+02	3.39281E+00
344	17030	9.02	35.12	1.40171E+01	1.51192E+02	7.65791E+00
344	17073	5.48	35.15	1.11361E+01	1.75971E+02	7.50590E+00
344	17110	1.94	36.73	8.18763E+00	1.62504E02	7.46846E+00
344	62131	32.84	35.37	5.96509E+01	2.92760E01	5.38266E+00
344	62071	36.33	36.15	3.70373E+01	5.9183 3E+01	4.52041E+00
344	61951	43.26	38.37	3.71135E+01	7.97472E+01	7.62423E+00
345	16399	26.58	35.17	4.3150 E+01	1.03035E+02	5.98715E+00
345	13340	23.10	35.59	1.22967E+01	1.12850E+02	6.22380E+00
345	16279	19.50	36.92	2.0167 E+01	1.29541E+02	6.64039E+00
345	16230	16.92	37.78	1.1983 E+01	1.61434E+02	7.22981E+00
345	16159	12.42	38.65	8.56797E+01	1.86430E+02	8.00038E+00
345	15110	6.94	39.43	5.21386E+01	1.73403E+02	7.82499E+00
345	15100	5.94	39.43	5.21386$+01	1.73403E+02	7.52499E+00
346	15630	41.81	34.65	2.20224F+01	1.03642E+02	3.56525E+00
346	15570	38.30	35.85	1.50162E+01	6.77709E+01	3.33122E+00
346	15513	34.78	37.82	1.11962E+01	7.46397E+01	4.56235E+00
346	15450	31.26	35.13	1.90649E+01	1.55666E+02	4.96032E+00
346	15330	37.73	39.08	1.37780E+01	1.72846E+02	5.5648 E+00
346	55815	64.73	34.83	3.36457E+01	1.09212E+02	3.68752E+00
346	59630	.52	35.55	1.53229E+01	1.32179E+02	7.75186E+00
346	59510	7.51	37.48	9.67528E+01	1.54611E+02	7.67298E+00
346	51450	41.01	38.00	1.11903E+01	1.76736E+02	7.69636E+00
346	50390	14.51	38.85	2.3320.E+01	1.19030E+02	7.49084E+00
347	14762	51.13	35.03	1.6508E+01	6.75764E+01	2.52155E+00
347	14702	47.66	36.83	1.30183E+01	6.71774E+01	4.04030E+00
347	14642	44.18	38.01	1.41732E+01	1.13365E+02	3.93475E+00
347	14582	40.68	39.40	2.55860E+01	1.19505E+02	3.95786E+00
348	15874	59.15	34.72	1.54733E+01	9.42248E+01	2.72361E+00
348	13814	55.74	36.93	5.50 25E+01	8.93579E+01	3.10741E+00
349	12242	56.96	39.18	4.74423E+01	1.12529E+02	2.74313E+00
349	12842	56.96	39.18	4.74423E+01	1.12529E+02	2.74313E+00
351	16337	27.27	35.47	1.15622E+01	1.70015E+02	5.29117E+00
351	16277	23.74	36.42	9.98651E+01	1.11337E+02	8.33637E+00
351	16217	20.20	37.34	1 75562E+01	1.29303E+02	6.48838E+00

TABLE 3 - ESTIMATES FOR ENTIRE "MOSCOW" FILE Cont'd

TIME	LAT.	LONG(E)	σ_N^2	σ_T^2	f_0F2
351 15697	13.11	35.08	8.50366E+00	1.95455E+02	7.01399E+00
351 91234	15.25	36.02	2.59007E+01	9.49846E+01	7.36896E+00
351 51233	21.79	36.92	1.56326E+01	1.26278E+02	7.02330E+00
351 51164	25.22	37.82	2.54269E+01	1.05310E+02	5.09726E+00
351 51104	28.70	38.73	4.53723E+01	7.73601E+01	4.08549E+00
352 15558	41.92	35.22	7.23676E+01	1.62256E+02	4.97639E+00
352 15498	38.42	36.45	9.32173E+01	1.71519E+02	4.89868E+00
352 15378	31.38	38.65	2.35431E+01	1.50802E+02	4.96963E+00
352 50552	1.03	36.25	1.34844E+01	1.58076E+02	6.55220E+00
352 60492	4.52	37.05	1.93312E+01	1.89487E+02	6.91073E+00
353 14846	48.71	36.82	5.24226E+01	4.68910E+01	2.74888E+00
353 14587	45.29	38.27	4.48764E+01	8.02098E+01	7.92825E+00
354 63614	57.57	38.08	5.51275E+01	7.02488E+01	3.44156E+00
354 63614	57.57	38.08	5.51275E+01	7.02488E+01	3.44156E+00
355 12668	60.58	35.10	1.55722E+01	1.80019E+02	3.24164E+00
355 12809	61.30	38.04	1.01646E+01	1.66823E+02	2.18328E+00
355 12809	61.30	38.04	1.31646E+01	1.86823E+02	2.18328E+00
355 62854	42.28	35.04	5.33527E+01	4.38454E+01	4.99976E+00
355 62794	45.73	36.38	5.35578E+01	6.05517E+01	3.86391E+00
355 62734	49.16	37.85	4.32224E+01	5.89715E+01	2.71875E+00
356 17865	13.37	35.29	8.54848E+00	1.47652E+02	7.63929E+00
356 16995	9.82	36.14	1.68764E+01	1.51839E+02	7.09862E+00
356 16935	6.27	36.97	1.80689E+01	1.44672E+02	7.18106E+00
356 16875	2.72	37.79	1.11813E+01	1.78000E+02	7.47577E+00
356 62070	28.18	34.89	4.30368E+01	1.05263E+02	4.55410E+00
356 62010	31.66	36.88	4.46649E+01	9.98143E+01	4.46840E+00
356 81950	35.12	36.94	4.21797E+01	1.00588E+02	5.09726E+00
356 81890	38.58	38.77	4.48806E+01	6.20640E+01	4.02168E+00
356 61830	42.04	39.28	3.73194E+01	5.61991E+01	3.85482E+00
357 11919	70.41	36.21	3.80145E+01	1.53902E+02	3.52045E+00
357 18928	31.18	34.97	2.82707E+01	1.15883E+02	4.45373E+00
357 16288	27.65	35.98	1.76679E+01	1.26297E+02	5.24590E+00
357 16288	24.12	36.93	8.62161E+01	1.11030E+02	5.878 4E+00
357 16388	17.03	38.73	1.09000E+01	1.92891E+02	7.29007E+00
357 61337	11.08	34.85	2.20309E+01	1.62636E+02	6.90142E+00
357 61276	14.60	35.70	1.65941E+01	1.66018E+02	7.52097E+00
357 61217	18.03	36.55	8.18587E+00	1.74436E+02	7.10793E+00
357 61097	24.03	38.35	2.31868E+01	1.17365E+02	5.02413E+00
357 61037	28.46	39.30	3. 5111E+01	5.79547E+01	4.37435E+00
359 11626	51.90	35.91	2.43723E+01	1.15588E+02	3.61715E+00
359 14566	43.44	37.54	4.5515 E+01	8.23848E+01	3.50809E+00
359 145 6	44.97	39.00	5.16178E+01	1.13637E+02	3.72121E+00

TABLE 4 - ESTIMATES FOR ENTIRE "BOULDER" FILE

TIME	LAT.	LONG(E)	σ_N^2	σ_T^2	f_0F2
358 65471	84.68	35.71	4.14545E+01	1.05924E+02	3.32324E+00
359 54509	50.97	36.78	5.13 3 E+01	8.81326E+01	3.14110E+00
360 23721	5 .96	36.27	1.27909E+01	1.23 57E+02	2.30132E+00
361 13650	55.50	3 .29	6. 6 65E+01	3.96223E+01	2.39966E+00
361 13660	55.60	3 .29	6.46865E+01	3.96223E+01	2.39966E+00
361 63634	52.35	35.66	4.67911E+01	5.22124E+01	3.72696E+00
360 63574	55.74	37.53	4.24673E+01	7.326 9E+01	2.88567E+00
361 62719	45.88	37.04	4.10123E+01	4.82876E+01	3.85450E+00
361 62660	49.25	36.49	4.2131 E+01	4.63439E+01	3.45088E+00
362 17042	17.12	34.99	1.57749E+01	1.13748E+02	6.09892E+00
362 15982	13.58	35.66	1.35996E+01	1.42249E+02	7.24488E+00
362 16922	10.03	36.70	1.35096E+01	1.73465E+02	7. 6274E+00
362 16862	6.48	37.53	1.45558E+01	1.92047E+02	7.91894E+00
362 168 2	2.93	38.36	1.21875E+02	2.15418E+02	7.48153E+00
363 13615	68.69	39.20	4.49662E+01	1.37221E+02	4.06112E+00
362 52350	25.16	34.66	2.52736E+01	7.29772E+01	4.99538E+00
362 51990	28.65	35.62	4.37443E+01	5.05295E+01	4.61110E+00
362 61870	35.58	37.69	3.83937E+01	7.41369E+01	4.35007E+00
36 15466	45.39	35.11	7.33796E+01	1.81177E+02	1.08675E+00
364 5456	41.91	36.45	5.34439E+01	1.56155E+02	4.65054E+00
364 15345	38.41	37.67	3.69656E+01	1.36214E+02	3.89404E+00
364 15256	34.90	36.80	3.73475E+01	1.41351E+02	4.82693E+00

TABLE 4 - ESTIMATES FOR ENTIRE "BOULDER" FILE Cont'd

	TIME	LAT.	LONG(E)	σ_N^2	σ_T^2	σ^{F2}
347	13142	19.84	253.57	1.59348E+01	1.02440E+02	5.273132+00
348	50181	42.99	250.45	1.88665E+01	1.25561E+02	5.58389E+00
348	50081	35.98	232.83	1.50544E+01	1.38322E+02	7.07700E+00
348	500.1	32.45	253.90	1.92696E+01	1.72321E+02	6.09041E+00
349	49277	50.23	291.75	1.75017E+01	1.08824E+02	5.78883E+00
349	49217	46.75	253.30	2.21952E+01	1.23478E+02	5.70175E.00
349	3752	.55	251.73	1.17682E+01	7.05450E+01	7.11724E+00
349	37.3	3.99	252.58	1.11920E+01	8.81576E+01	6.14492E+00
349	36.3	7.48	252.40	1.35935E+01	1.01253E+02	7.35896E+00
350	54321	54.40	253.95	2.53037E+01	9.86235E+01	6.74940E+00
351	11897	53.06	25.03	1.53377E+01	1.377105+02	6.01728E+00
351	47471	51.46	257.51	1.52782E+01	9.921332+01	5.93287E+00
352	51713	16.43	250.17	1.12917E+01	7.65654E+01	7.09287E+00
352	51853	12.94	251.03	1.09246E+01	6.38553E-01	7.05343E+00
352	51533	3.39	251.63	8.25935E+01	6.19841E+02	6.95017E+00
352	51533	5.64	252.71	1.19701E+01	5.91074E+01	7.01974E+00
352	51473	2.29	253.53	8.85232E+00	6.03911E+01	7.35389E+00
352	11053	42.23	250.67	1.27686E+01	7.41206E+02	5.63797E+00
352	10327	45.68	242.63	1.54817E+01	1.16815E+02	5.54974E+00
353	13267	36.52	250.67	1.38723E+01	1.26935E+02	5.77188E+00
352	10257	12.45	251.84	1.12381E+01	1.82925E+02	5.82217E+00
352	10147	25.47	252.73	1.68341E+01	5.73178E+01	5.75050E+00
352	21057	20.92	252.14	1.03519E+01	1.23542E+02	5.03524E+00
352	51132	44.45	250.54	2121717E+01	9.22228E+01	6.08110E+00
354	50373	41.47	251.73	1.78043E+01	5.31435E+01	6.75872E+00
354	51203	40.37	422.37	2.22373E-01	1.37535E+01	5.22576E+00
355	13253	53.72	250.59	1.43248E+01	1.29043E+02	3.83829E+00
355	29143	26.82	292.11	1.02206E+01	1.32023E+02	3.44648E+00
355	6639	1.89	252.67	2.13414E+01	5.29198E+01	7.18602E+00
355	1549	1.72	253.64	1.67859E+01	4.48346E+01	7.43627E+00
355	5549	8.32	254.32	1.58804E+01	1.20811E+02	7.66723E+00
358	12716	12.76	121.47	1.74274E+01	1.43552E+02	8.37697E.00
358	10736	11.72	121.04	1.74204E+01	1.17593E+02	8.73603E.00
358	12575	37.05	234.13	1.82358E+01	9.05423E+01	8.47331E+00
358	24329	104.04	249.58	2.03537E+01	1.25957E+02	7.58102E-00
358	13257	48.52	245.97	1.73273E+01	9.12754E+02	5.41592E+00
358	13157	48.91	245.91	1.13797E+01	1.12139E+02	5.71512E+00
358	11527	52.94	250.61	1.27770E+02	1.27770E+02	5.50099E+00
358	27743	32.00	134.69	1.24126E+01	1.23072E+02	8.52365E+00
358	52421	2.97	249.97	1.28630E+01	6.01336E+01	7.11724E+00
358	31597	20.81	249.91	5.81023E+01	2.33073E+01	7.25995E+00
358	51637	18.47	250.73	6.23028E+02	7.45539E+01	7.29367E+00
358	51547	12.92	251.64	1.19205E+01	5.57930E+01	7.06918E+00
358	51457	5.82	253.32	9.78621E+00	7.18213E+01	7.02905E+00

TABLE 4 - ESTIMATES FOR ENTIRE "BOULDER" FILE Cont'd.

	TIME	LAT.	LONG (E)	σ_N^2	σ_T^2	f_0F2
358	51397	2.27	254.14	1.273818+01	5.40337E+01	2.24438E+00
359	13245	25.60	253.42	1.74483E+01	1.43225E+02	5.56480E+00
359	10153	29.04	251.35	2.27580E+01	1.43825E+02	3.82822E+00
359	10055	36.00	253.46	3.03558E+00	1.47470E+02	5.57412E+00
360	50103	47.37	243.52	1.99899E+01	1.11110E+02	5.57787E+00
360	50046	43.89	251.33	1.85216E+01	9.49214E+01	5.62287E+00
360	49956	14.74	252.82	1.48641E+01	9.39457E+01	5.57412E+00
360	8521	3.01	250.37	9.77685E+01	8.65833E+01	7.24488E+00
360	3481	11.43	291.13	1.35332E+01	1.17821E+02	7.48071E+00
360	94.1	14.98	252.23	1.83600E+01	1.02099E+02	5.57219E+00
360	9241	18.45	252.09	1.18383E+01	1.15613E+02	5.34791E+00
360	9231	21.94	253.78	1.76664E+01	1.12824E+03	5.45579E+00
360	24537	55.43	243.56	3.56555E+01	5.57232E+01	5.55221E+00
361	13564	66.58	254.18	3.23586E+01	5.24855E+01	6.57657E+00
361	49272	34.85	250.74	2.73834E+01	1.18733E+01	6.08488E+00
361	49142	51.11	252.54	2.23920E+01	1.05919E+02	4.82693E+00
362	12722	58.17	249.63	1.46371E+01	1.22839E+02	5.51885E+00
362	12652	59.73	252.03	1.71711E+01	1.01304E+02	6.01153E+00
362	48299	61.58	230.23	1.38212E+01	1.09843E+02	7.37320E+00
362	45328	58.24	252.80	2.14145E+01	1.15834E+02	7.338835+00
363	21829	43.70	252.15	2.75805E+01	1.40034E+02	5.62852E+00
363	11769	32.11	251.73	2.28504E+01	1.12570E+02	4.19806E+00
363	11709	55.38	256.64	2..33951E+01	1.70473E+02	7.29907E+00
363	47273	61.33	354.43	1.983063E-01	8.42635E+01	6.92579E+00
363	52413	2.07	249.55	1.14990E+01	6.24738E+01	6.95523E+01
363	52357	2.51	250.37	1.22313E+01	6.76357E+01	7.21119E+00
364	31511	12.47	251.42	1.35235E+01	7.29142E+01	7.14727E+00
364	51517	13.95	252.02	1.24423E+01	6.09076E+01	7.16660E+00
364	5144	10.32	252.85	1.37230E+01	5.57518E+01	7.05457E+00
364	51397	6.83	253.70	9.32366E+00	6.29071E+01	7.01574E+00
365	51790	31.72	351.67	1.78712E+01	1.02118E+02	6.19357E+00
365	31750	28.20	252.63	1.65124E+01	1.01718E+02	6.21804E+00
365	31570	24.58	253.64	1.54920E+01	1.50512E+02	7.76117E+00
365	45339	71.20	251.69	1.77602E+01	1.27502E+02	7.22883E+00
365	45339	71.20	251.69	1.77602E+01	1.27502E+02	7.]]882E+00

TABLE 5

RESULTS FOR MOSCOW WINDOW, WITH CRAMER-RAO BOUND AND SSIP VALUES

DAY	ISEC	DATE	LOCAL TIME	σ_N^2	σ_T^2	f_0 (MHz)	$\sqrt{CRB}$ (MHz)	SSIP
336	63845	Dec 2	19:44	44.06	95.04	3.211	0.47	2.3
337	62863	Dec 3	19:28	29.59	52.67	2.601	0.48	1.9
342	13886	Dec 8	5:51	30.43	113.21	3.269	0.36	2.7
343	62788	Dec 9	19:26	15.32	86.53	2.454	0.25	2.3
348	13814	Dec 14	5:50	56.04	89.36	3.107	0.56	1.8
354	63614	Dec 20	19:40	55.13	70.25	3.442	0.68	2.8
360	13660	Dec 26	5:48	64.69	39.62	2.400	0.98	2.0
360	63594	Dec 26	19:40	42.47	73.26	2.880	0.51	2.3

TABLE 6

RESULTS FOR BOULDER WINDOW, WITH CRAMER-RAO BOUND AND SSIP VALUES

DAY	ISEC	DATE	LOCAL TIME	σ_N^2	σ_T^2	$f_{0(MHz)}$	CRB (MHz)	SSIP
336	50316	Dec 2	6:59	32.82	100.77	5.717	0.52	3.3
336	50256	Dec 2	6:58	18.71	121.91	4.493	0.33	3.3
342	50215	Dec 8	6:57	21.51	102.96	5.854	0.42	4.4
346	11129	Dec 11	20:05	13.46	99.83	4.587	0.31	2.4
347	10142	Dec 12	19:49	18.95	102.44	5.373	0.38	2.8
352	11058	Dec 17	20:04	12.77	141.21	5.638	0.30	2.8
353	10087	Dec 18	19:48	11.35	123.84	6.075	0.31	2.7
354	50073	Dec 20	6:55	23.89	120.01	5.805	0.41	4.0
354	50013	Dec 20	6:53	17.80	93.15	6.759	0.44	4.0
360	49986	Dec 26	6:53	10.88	93.95	5.574	0.32	3.2

FIGURE 1a

COUNTS FOR COMPLETE MOSCOW FILE

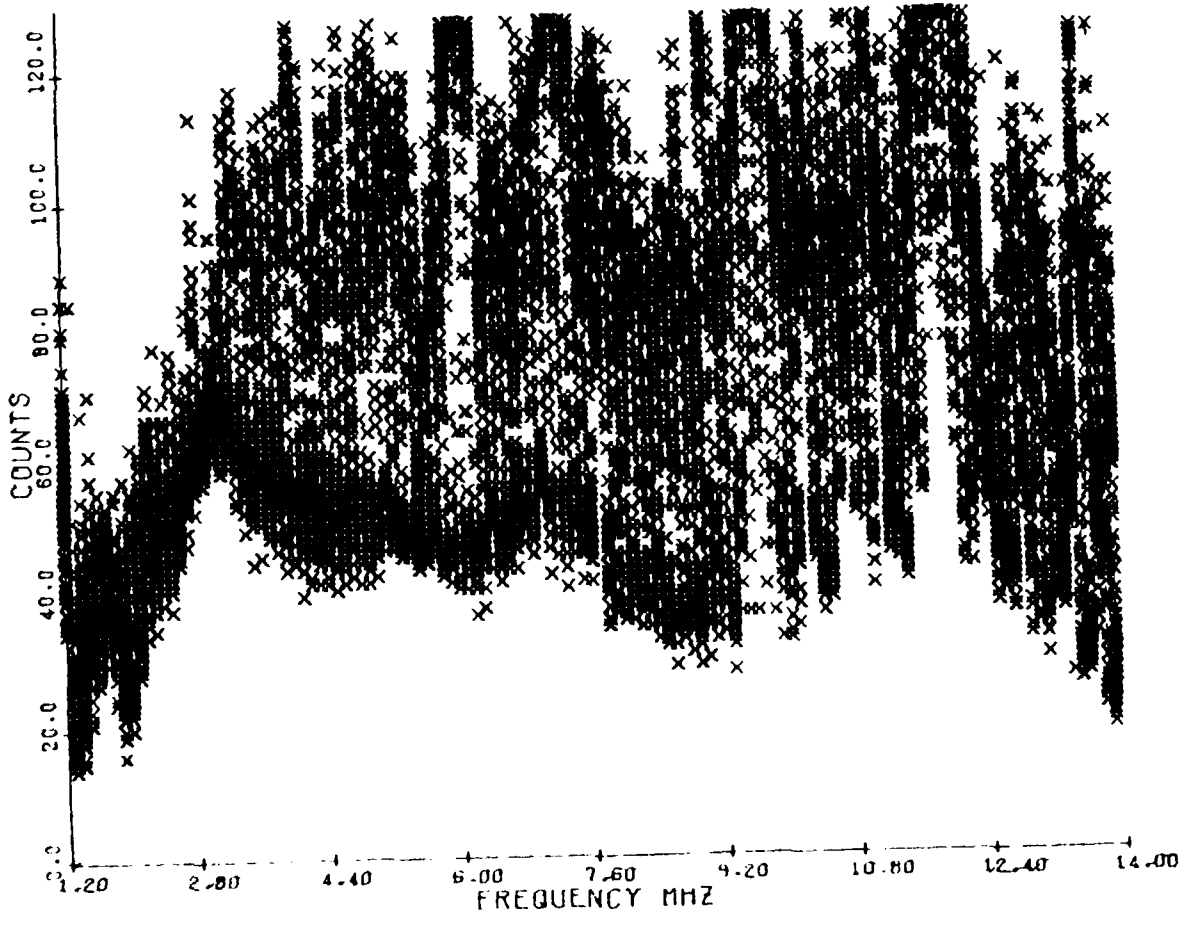

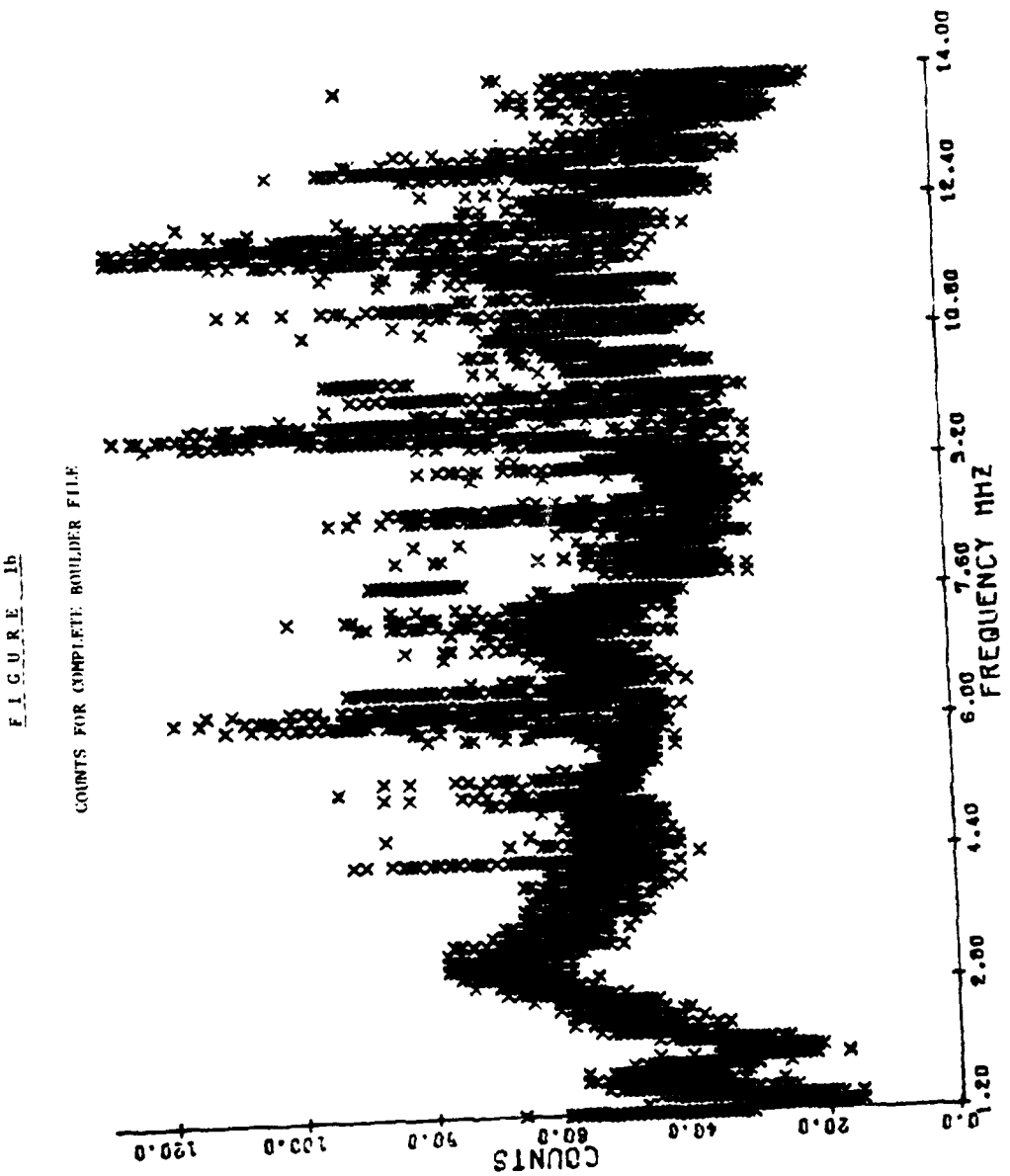

FIGURE 1b

COUNTS FOR COMPLETE BOULDER FILE

FIGURE 2a

COUNTS FOR 5° SQUARE CENTERED OVER MOSCOW

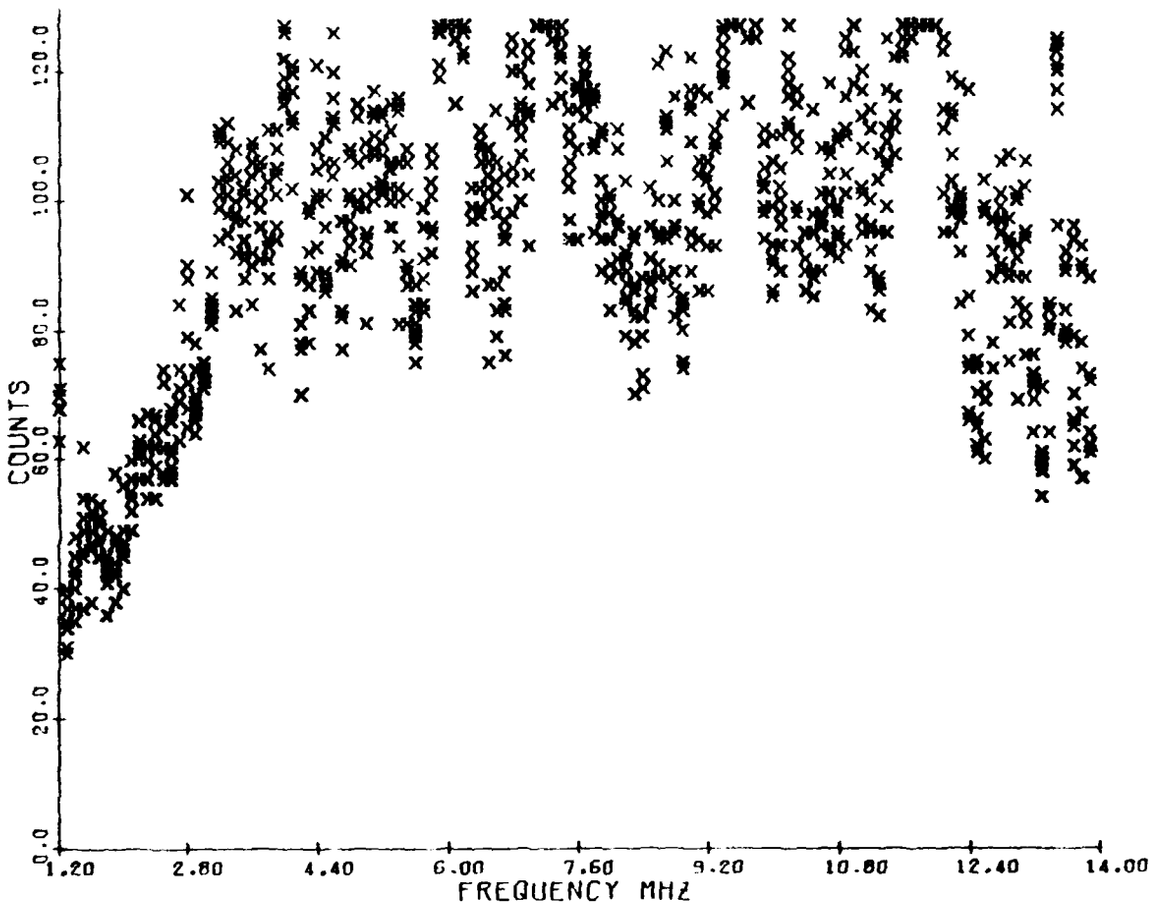

FIGURE 2b

COUNTS FOR 5° SQUARE CENTERED OVER BOULDER

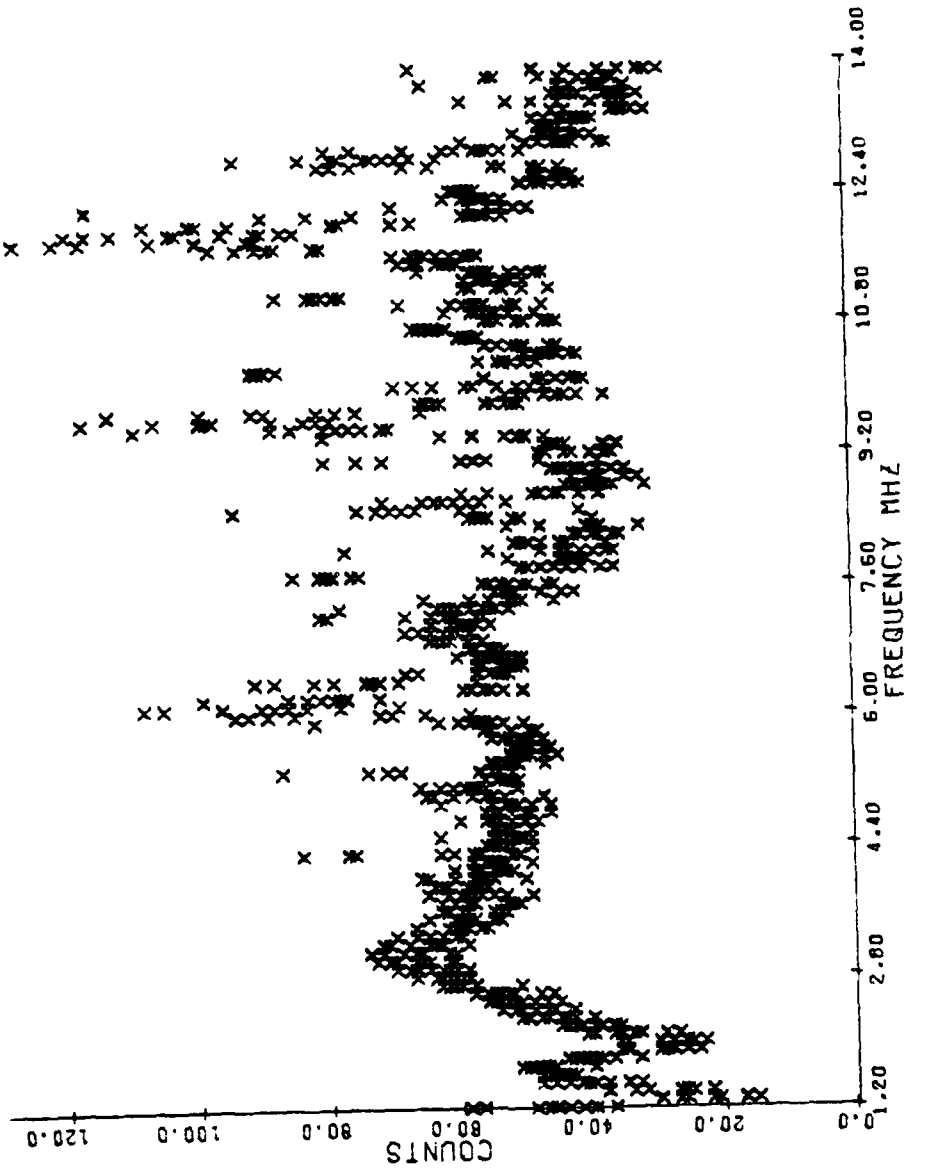

MOSCOW 1

Figure 3a

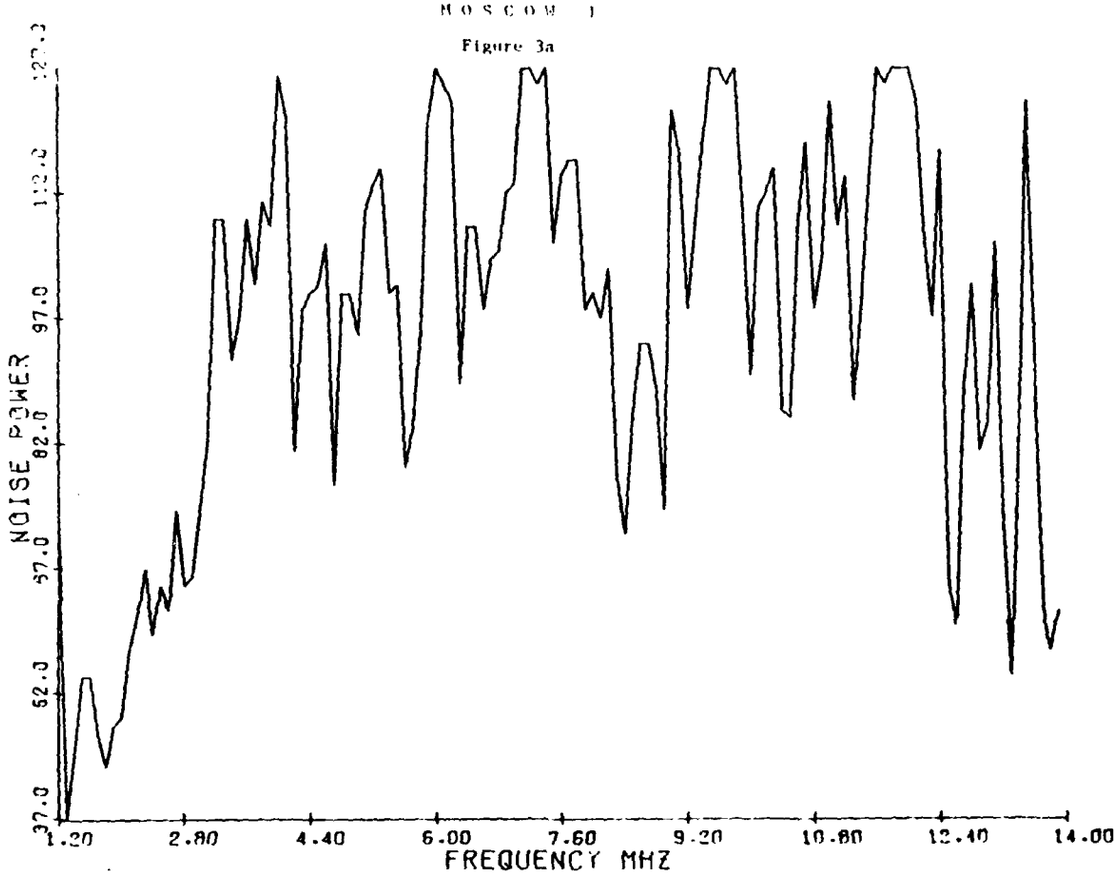

MOSCOW 1

Figure 3b

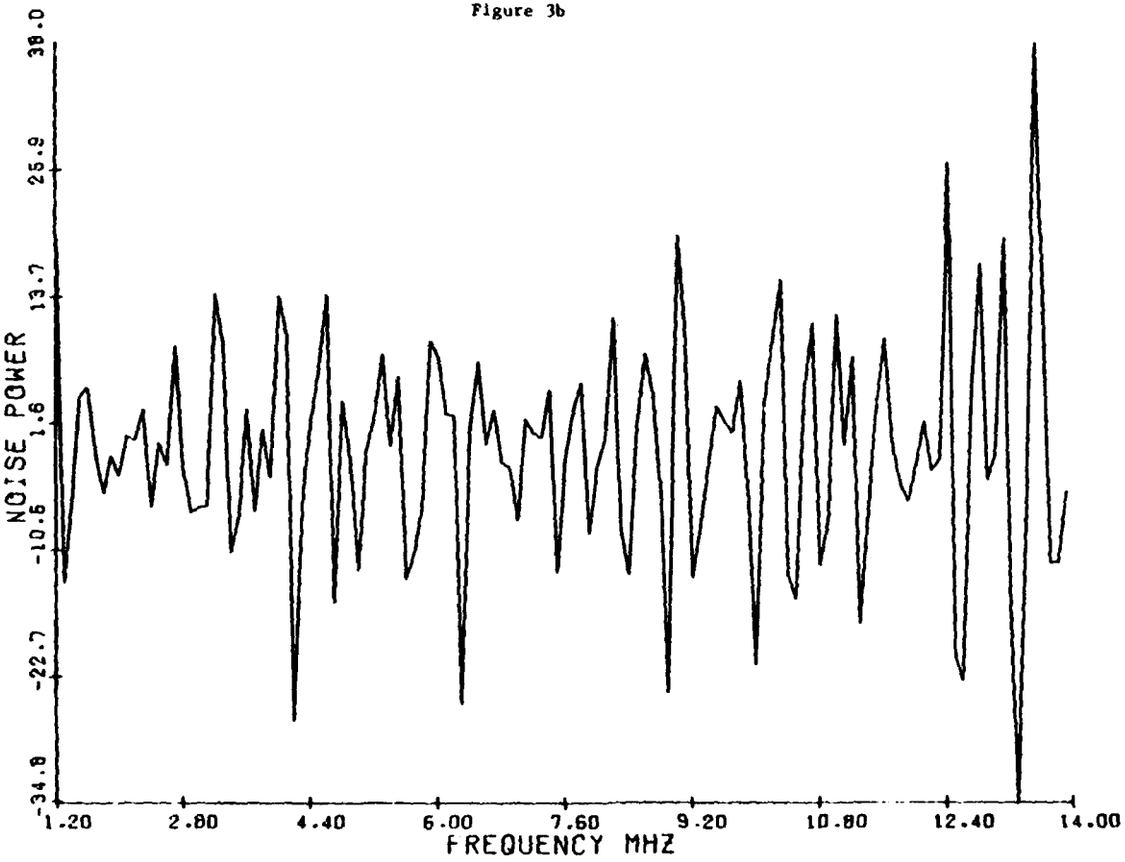

MOSCOW 1

Figure 3c

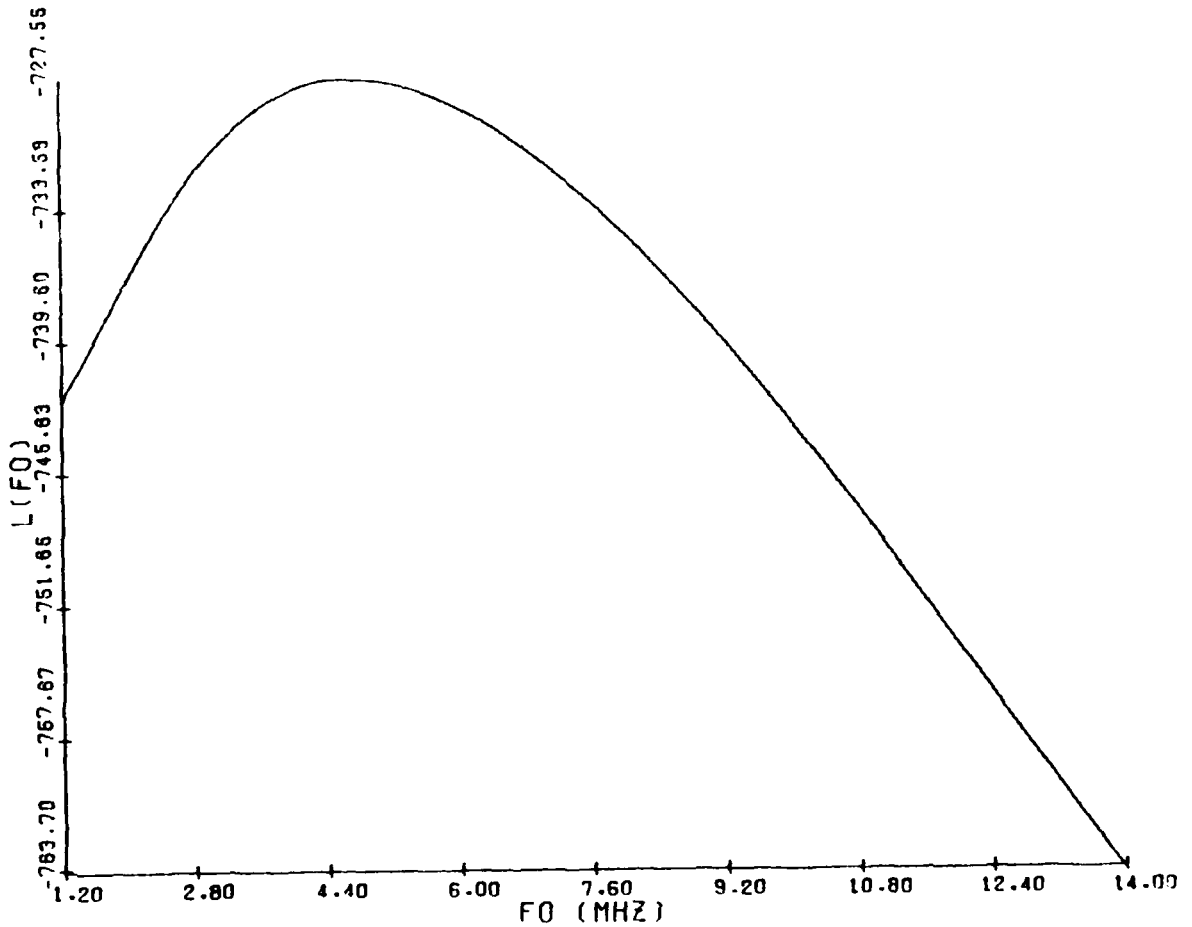

MOSCOW 1

Figure 3d

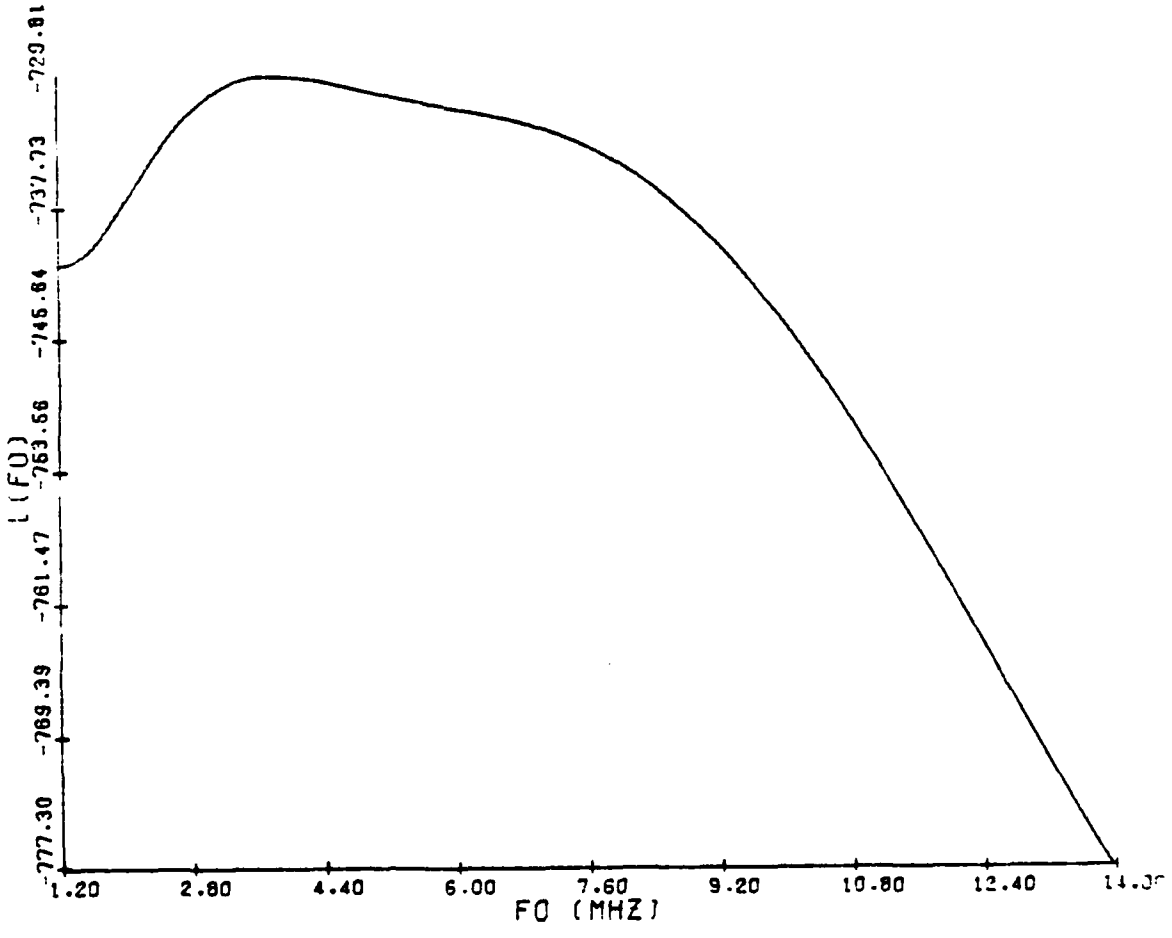

MOSCOW 1

Figure 3e

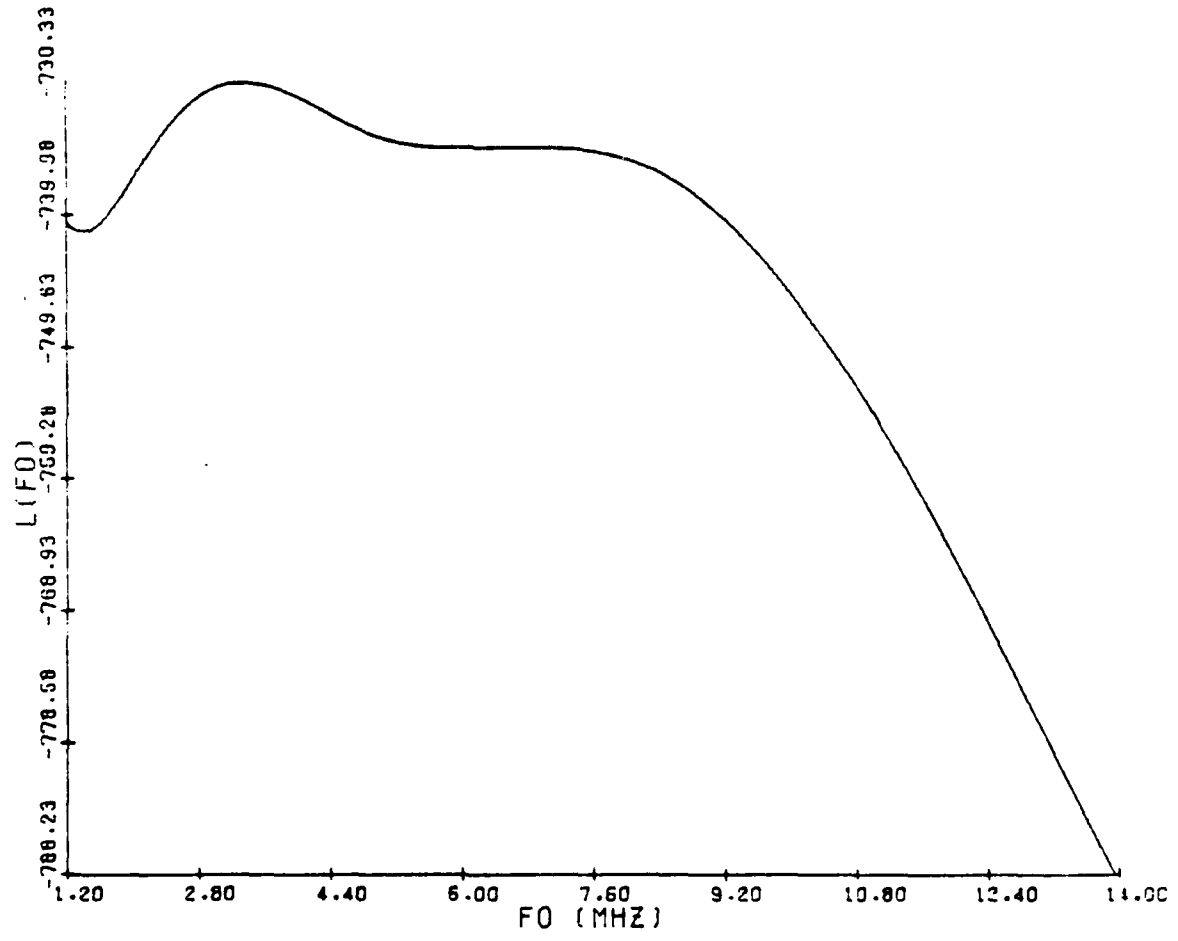

MOSCOW 1

Figure 3f

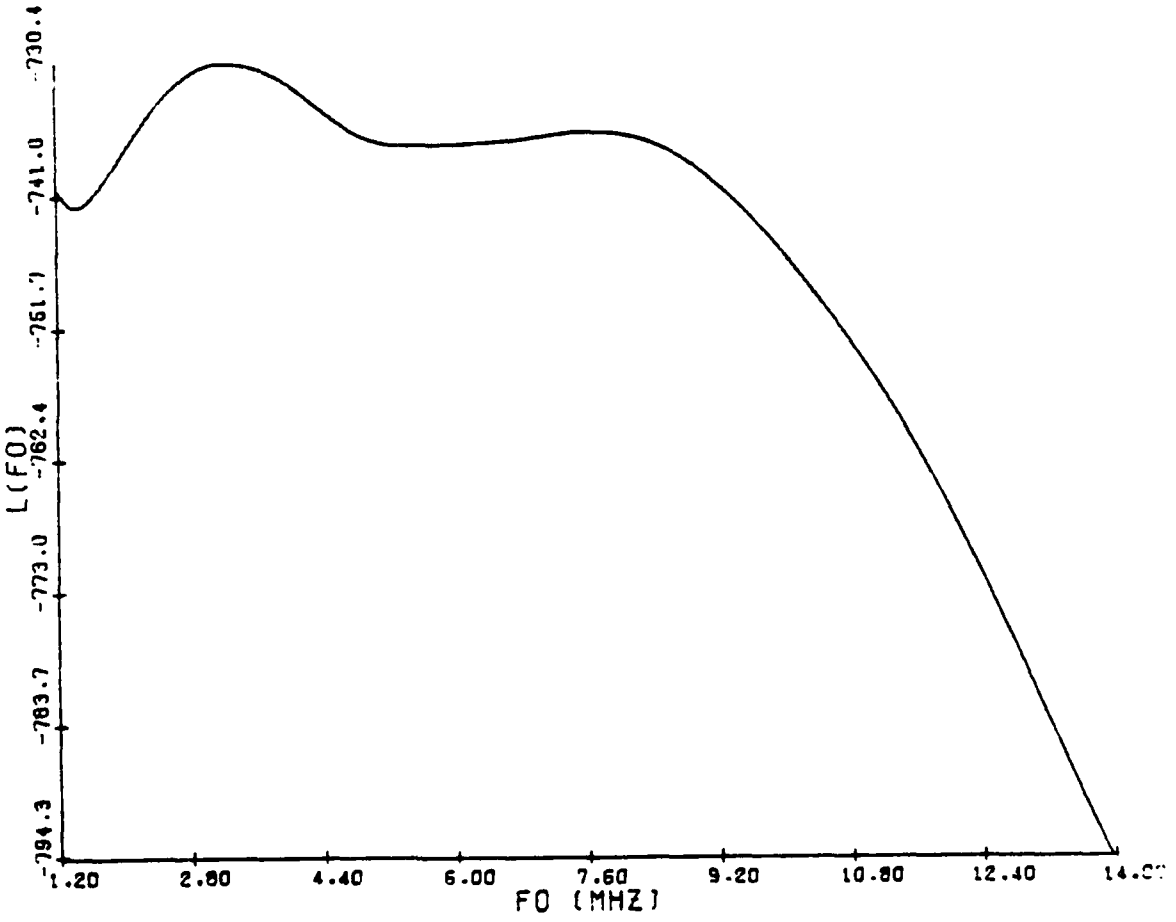

MOSCOW 1

Figure 3g

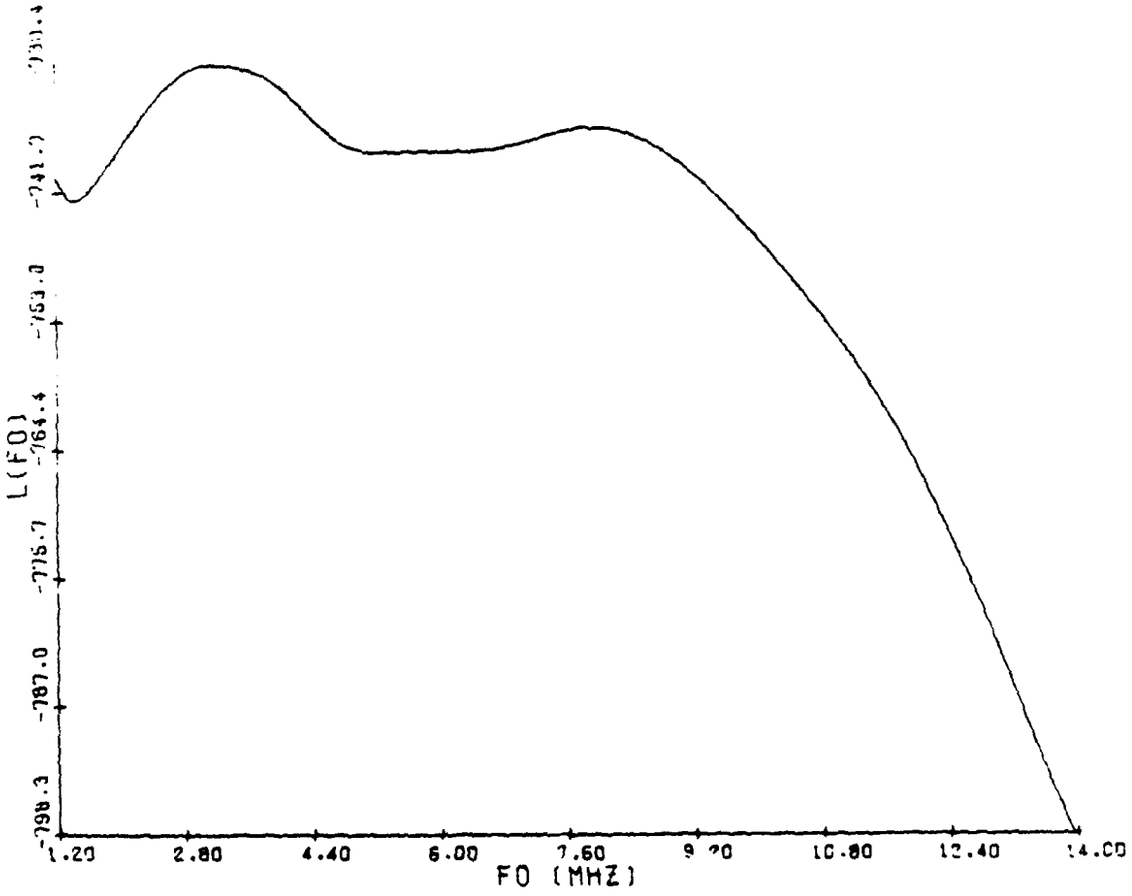

BOULDER - 50316

Figure 4a

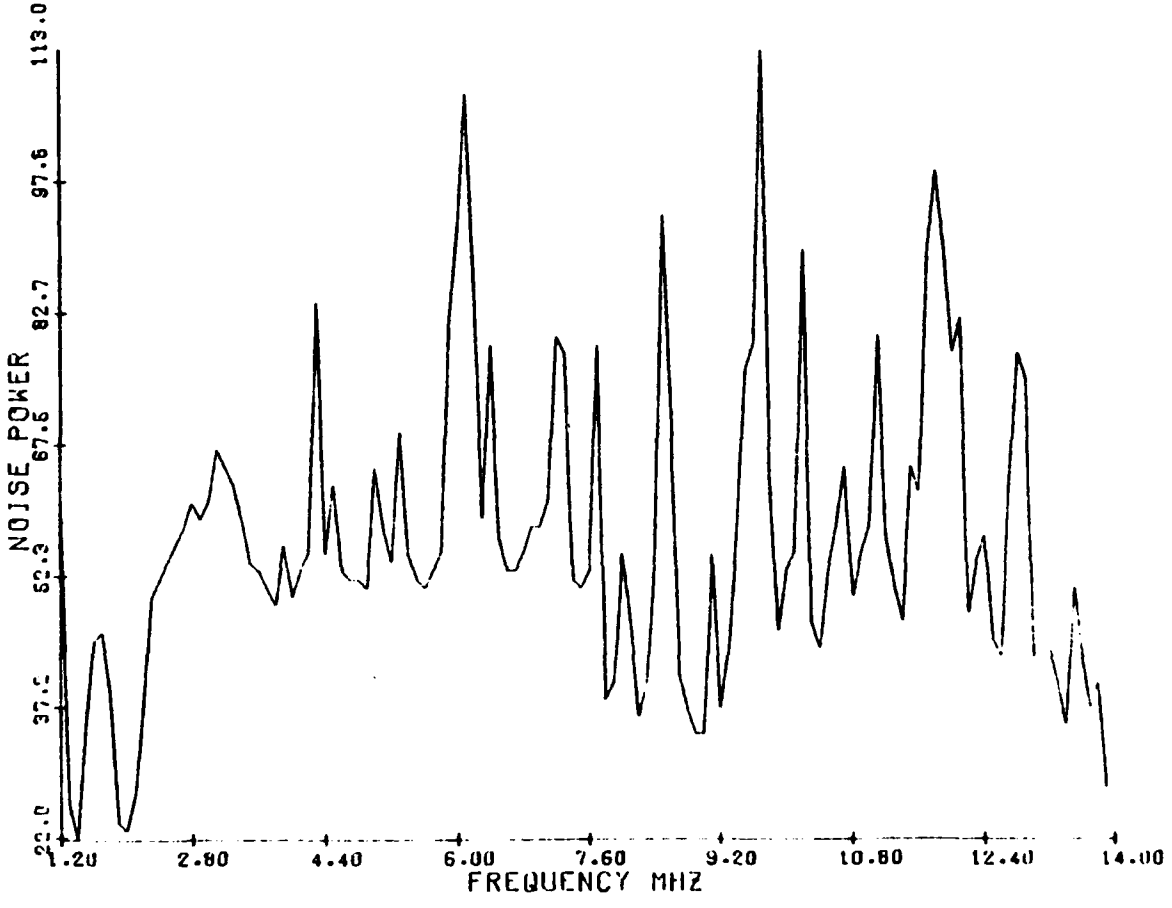

BOULDER - 50316

Figure 4b

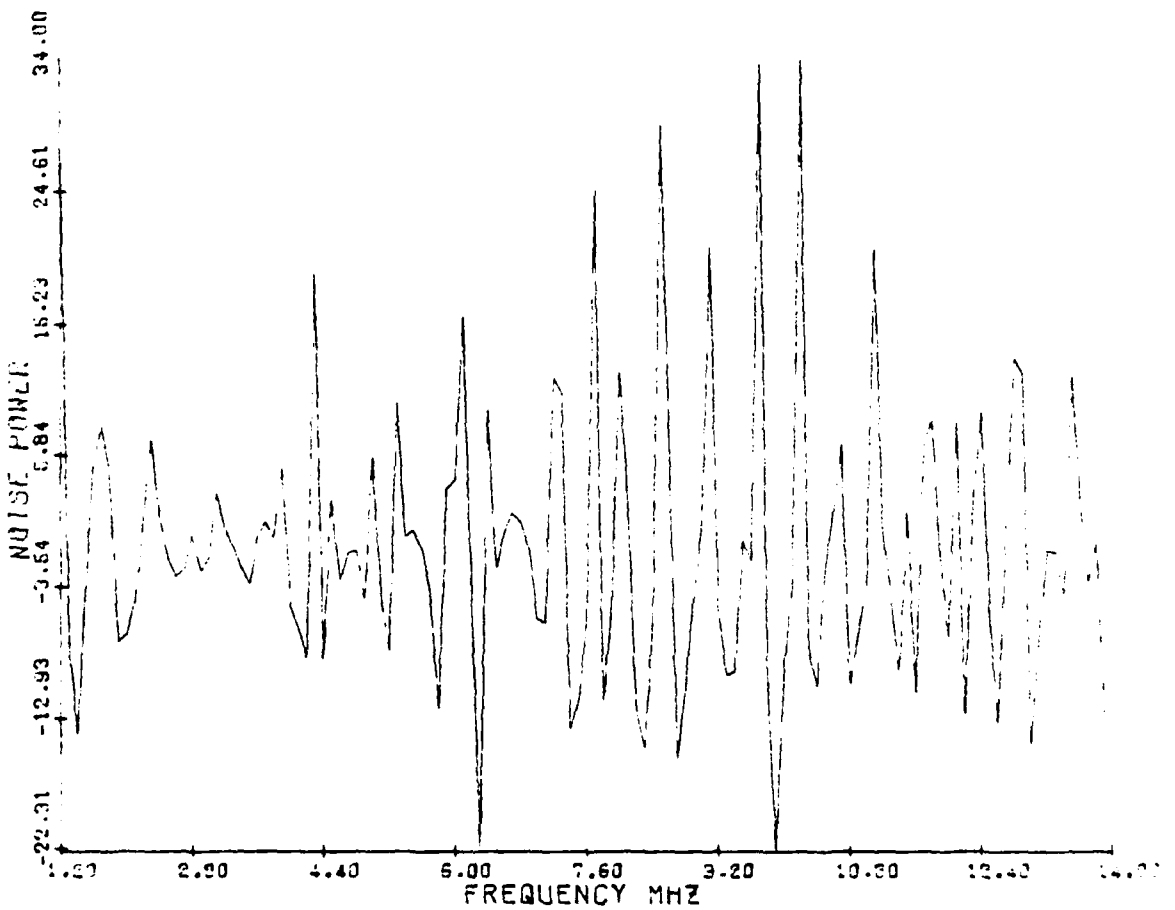

BOULDER - 50316

Figure 4c

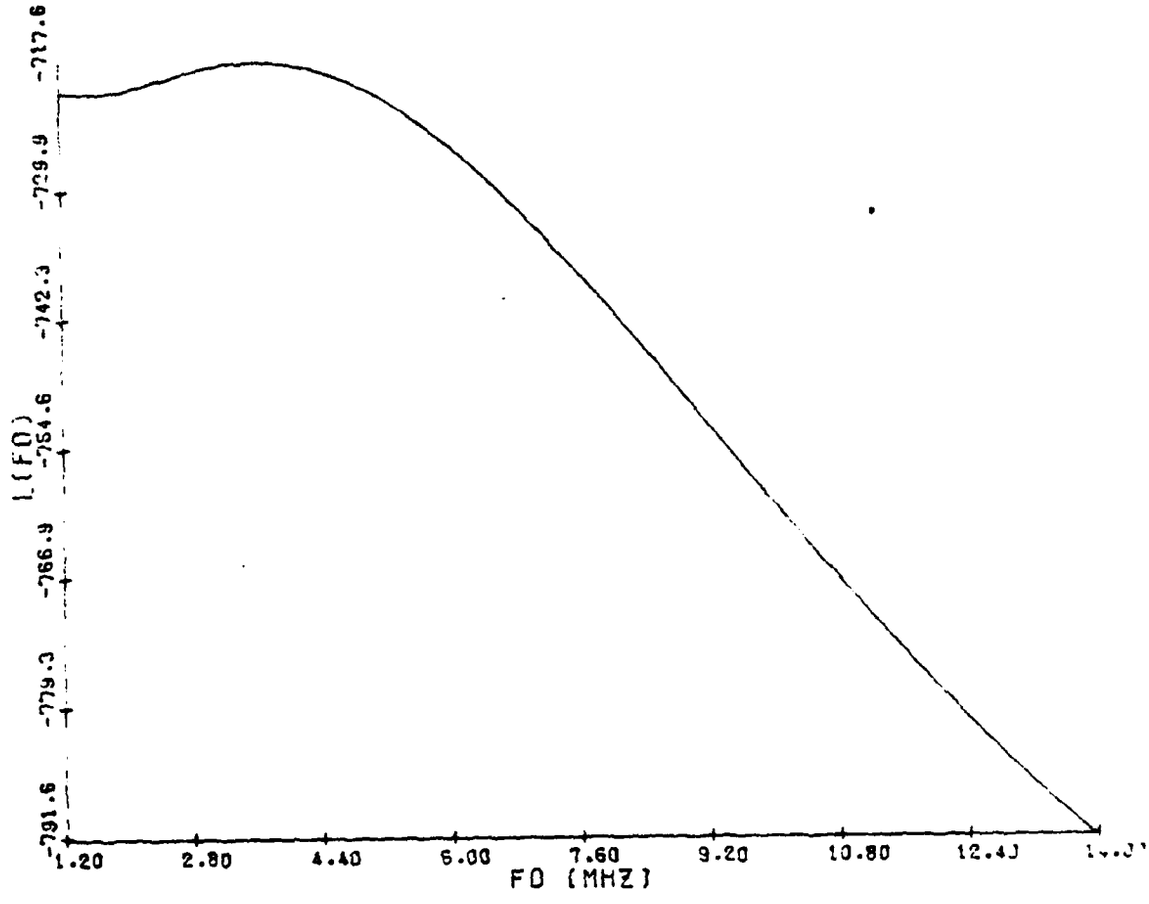

BOULDER - 50316

Figure 4d

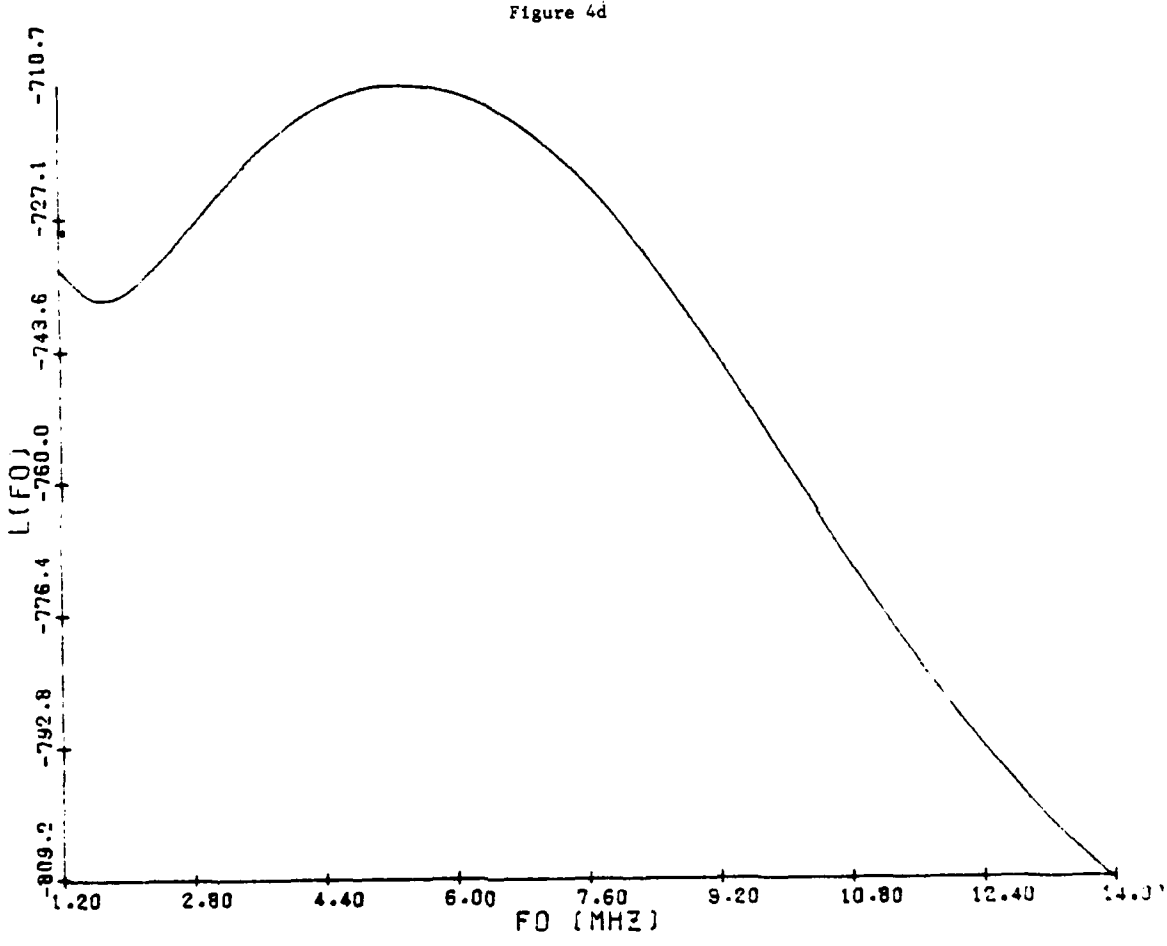

BOULDER - 50316

Figure 4e

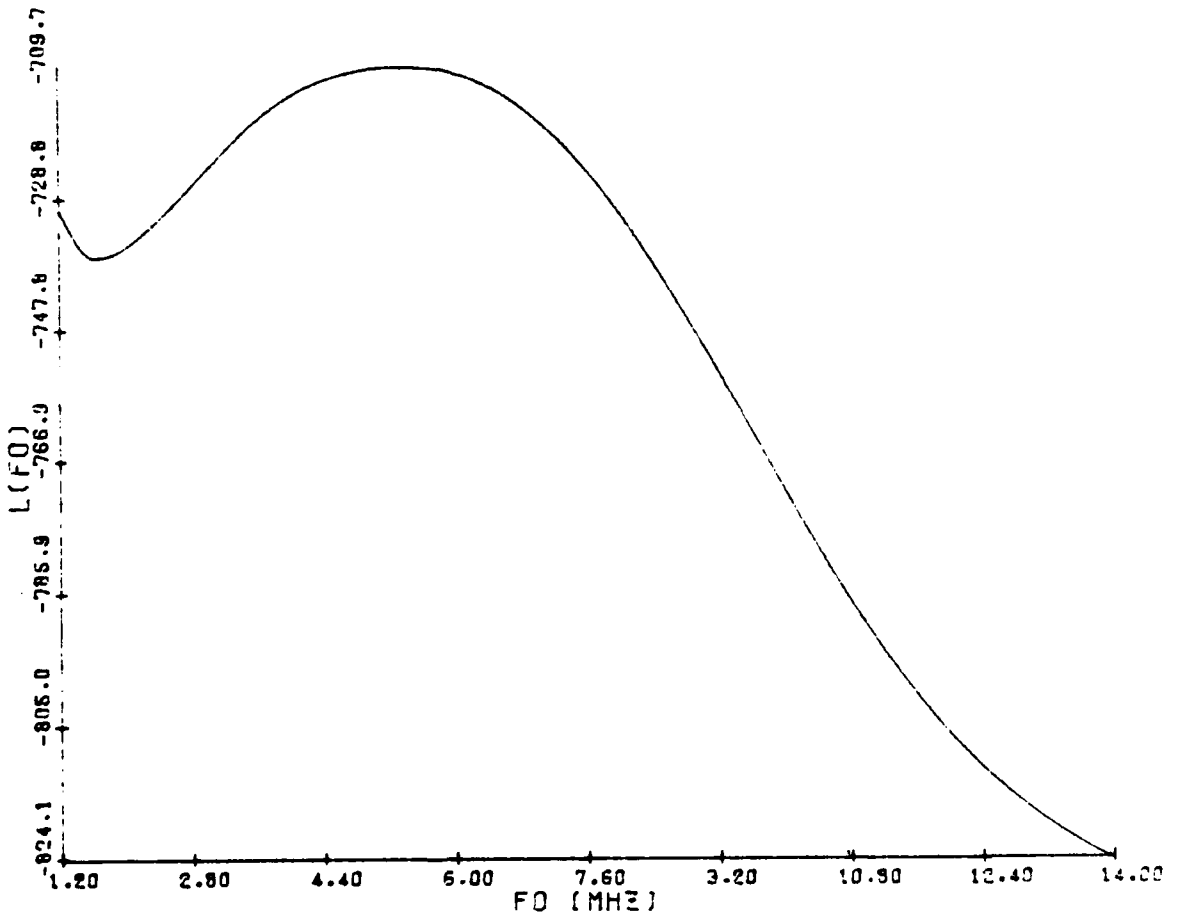

BOULDER - 50316

Figure 4f

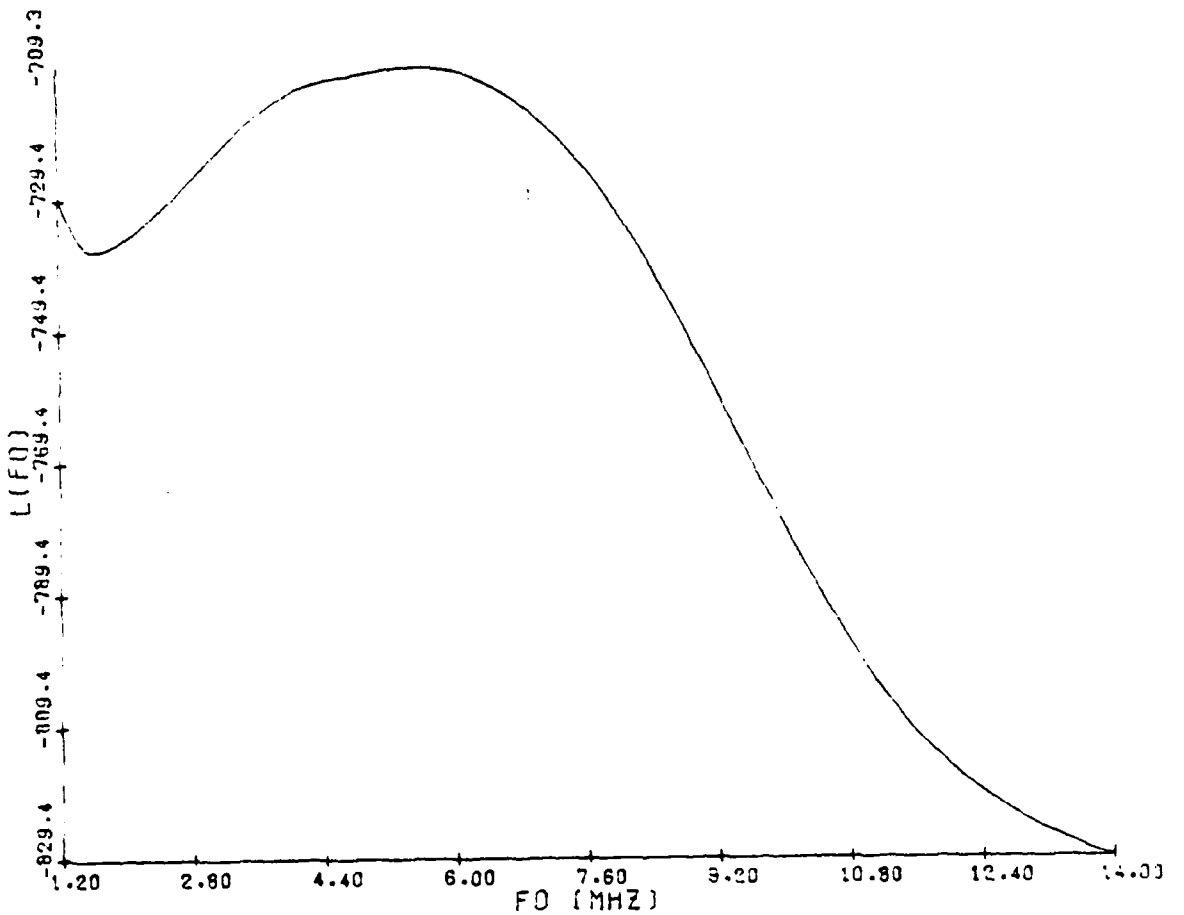

BOULDER - 50316

Figure 4g

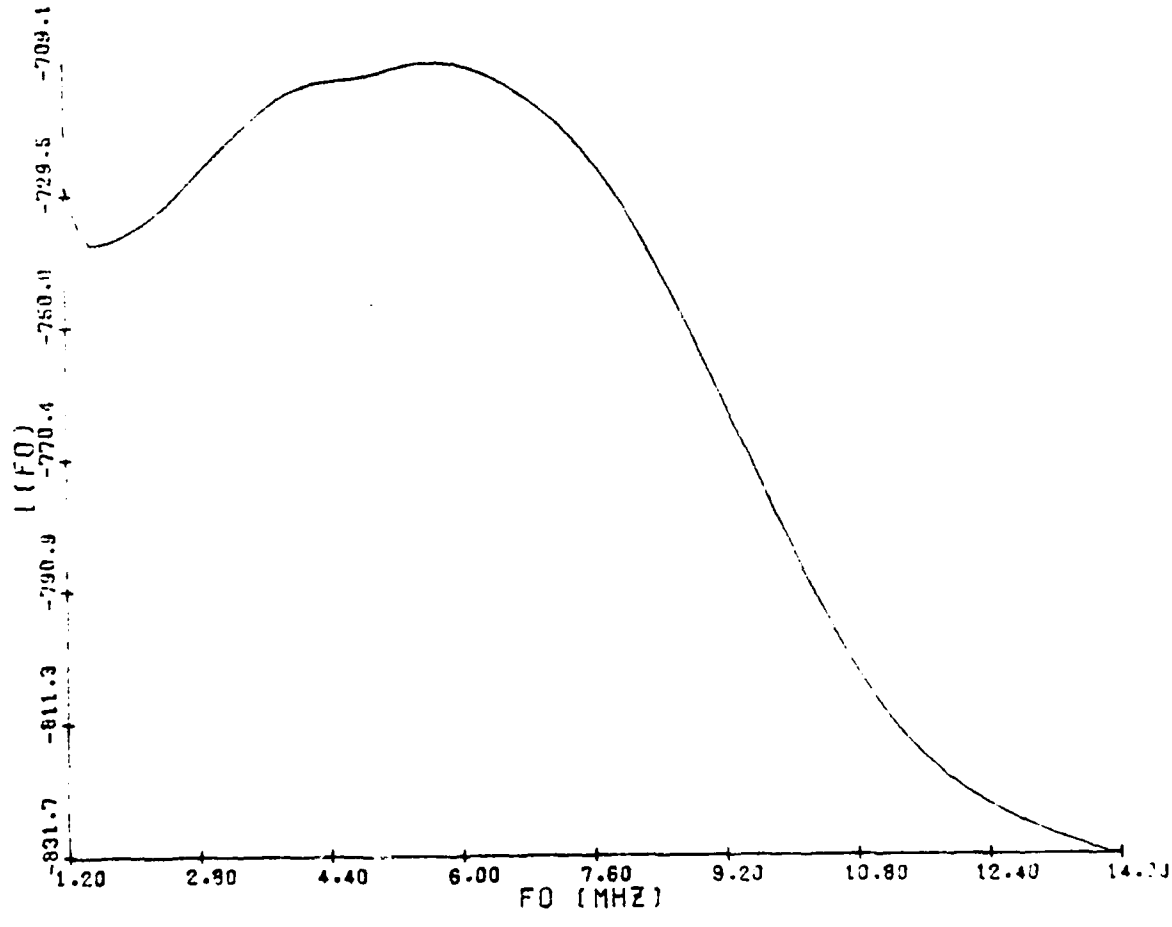

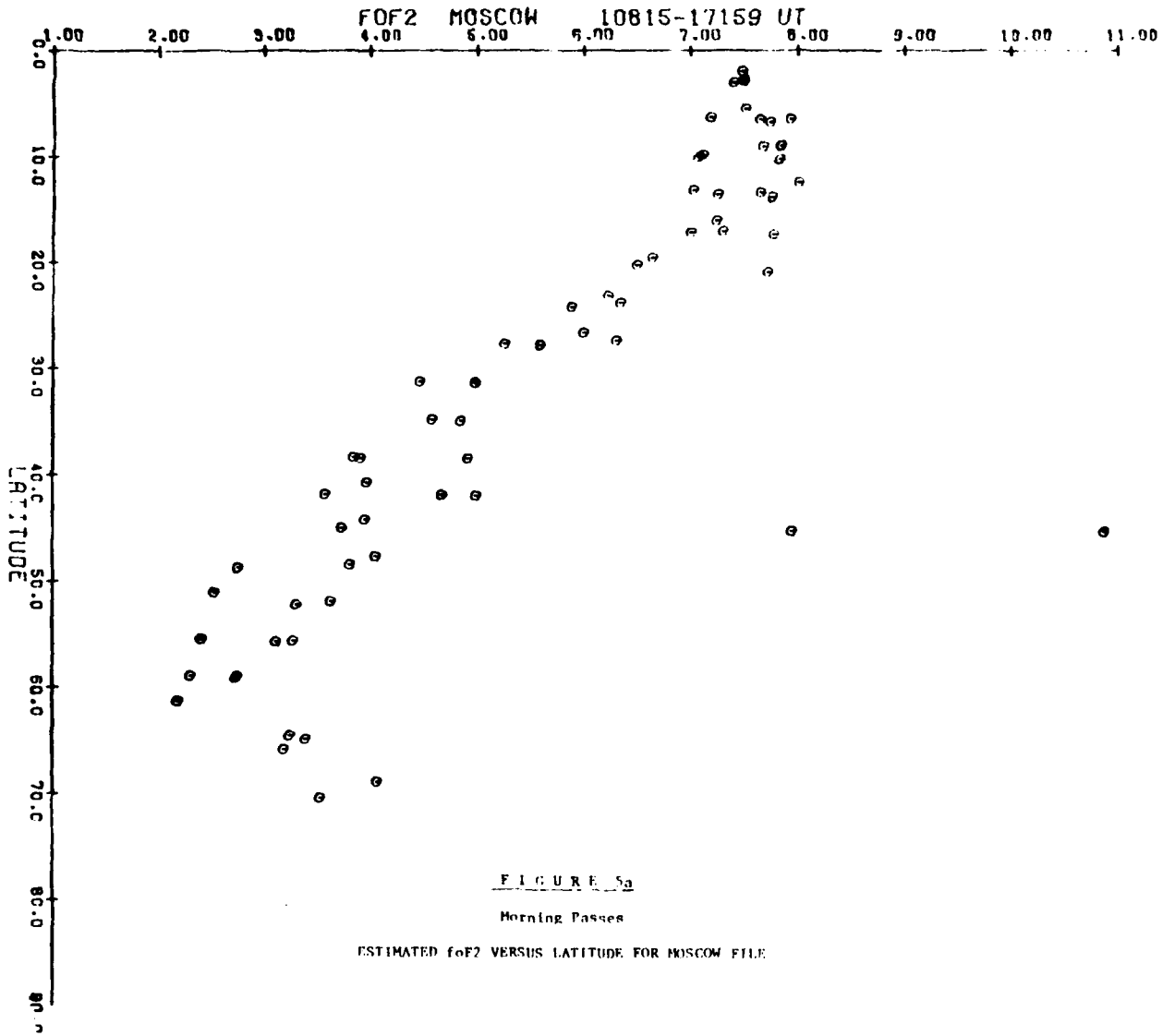

FIGURE 5a

Morning Passes

ESTIMATED foF2 VERSUS LATITUDE FOR MOSCOW FILE

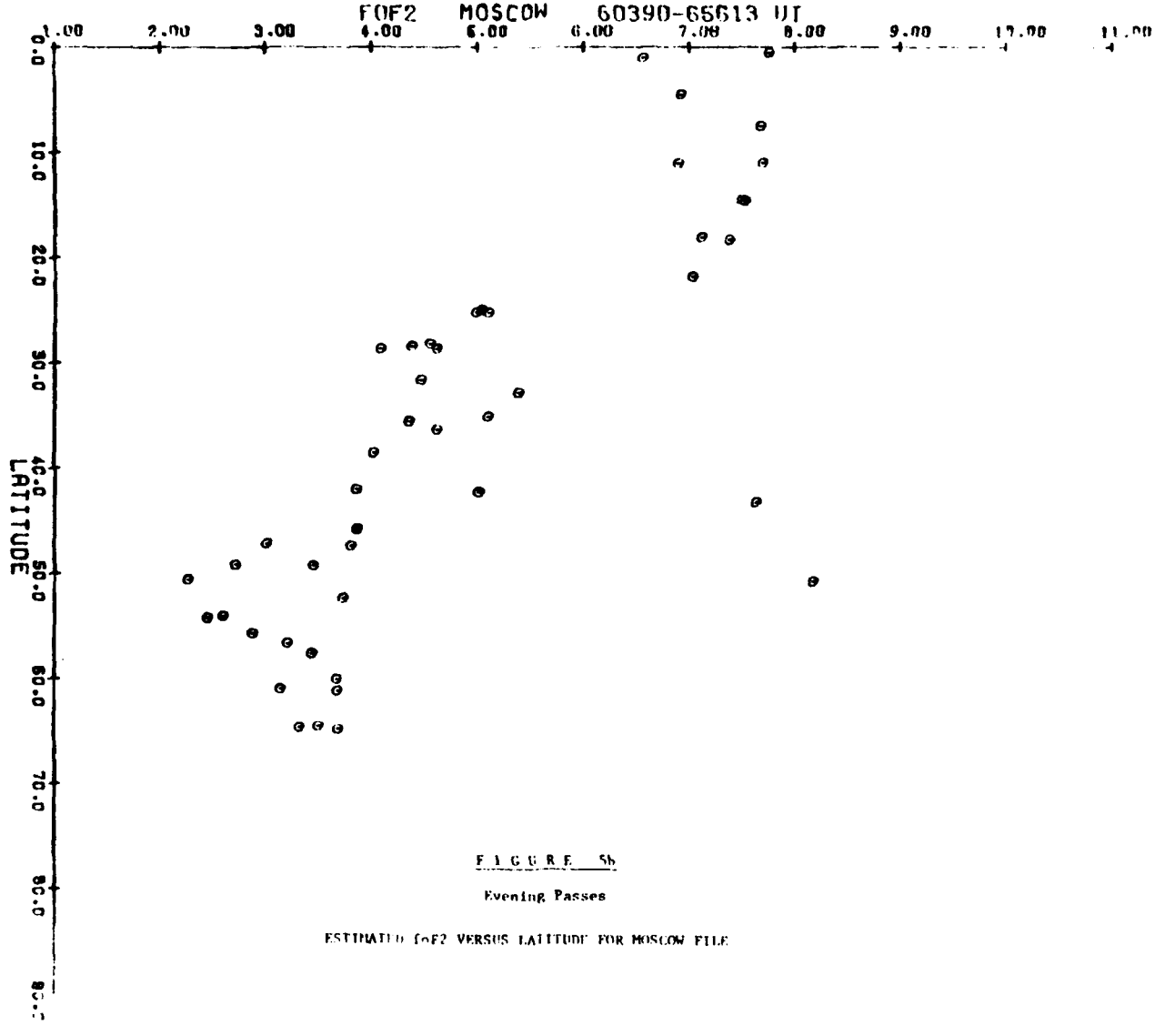

FIGURE 5b

Evening Passes

ESTIMATED foF2 VERSUS LATITUDE FOR MOSCOW FILE

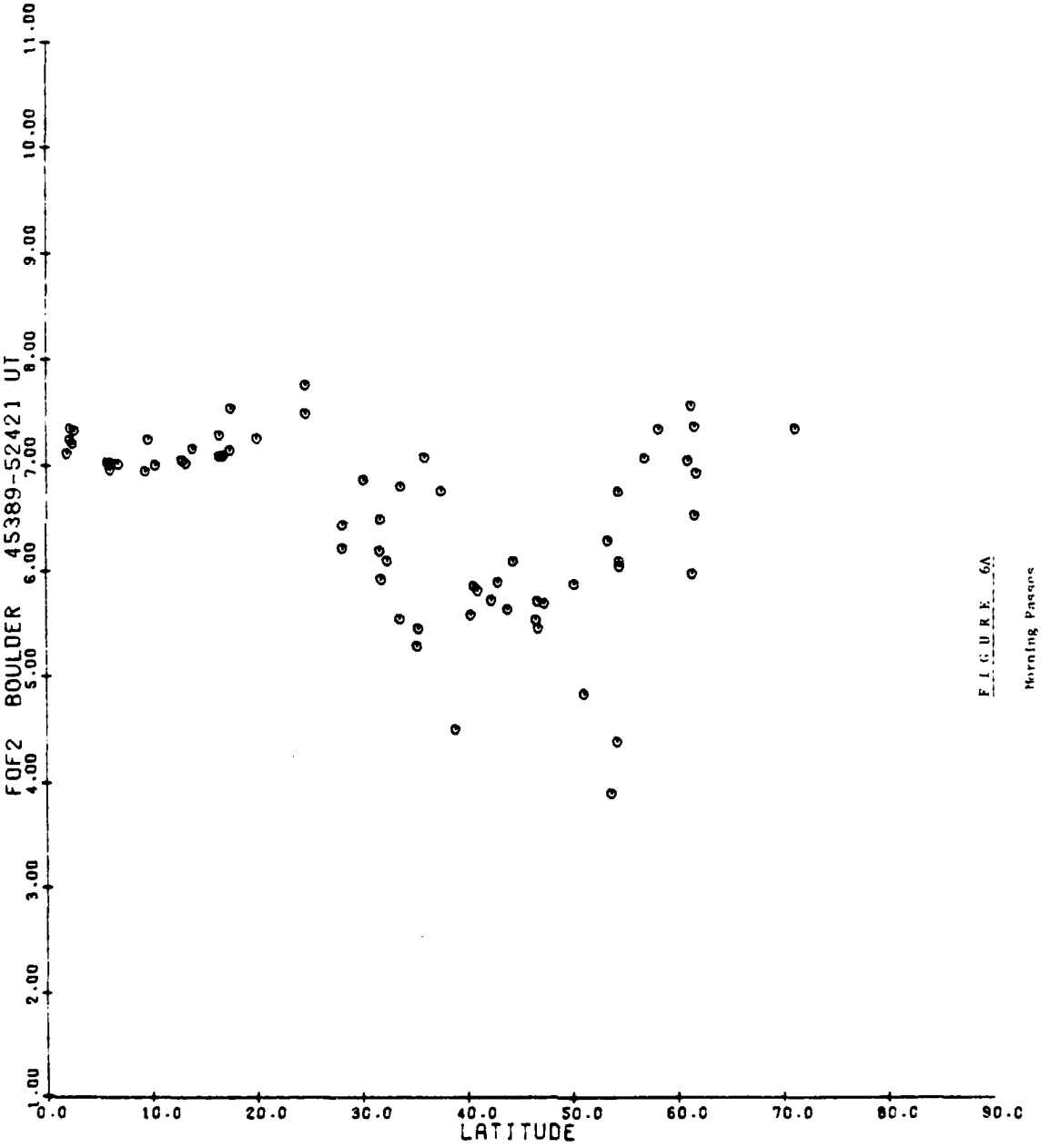

FIGURE 6A

Morning Passes

ESTIMATED foF2 VERSUS LATITUDE FOR BOULDER FILE

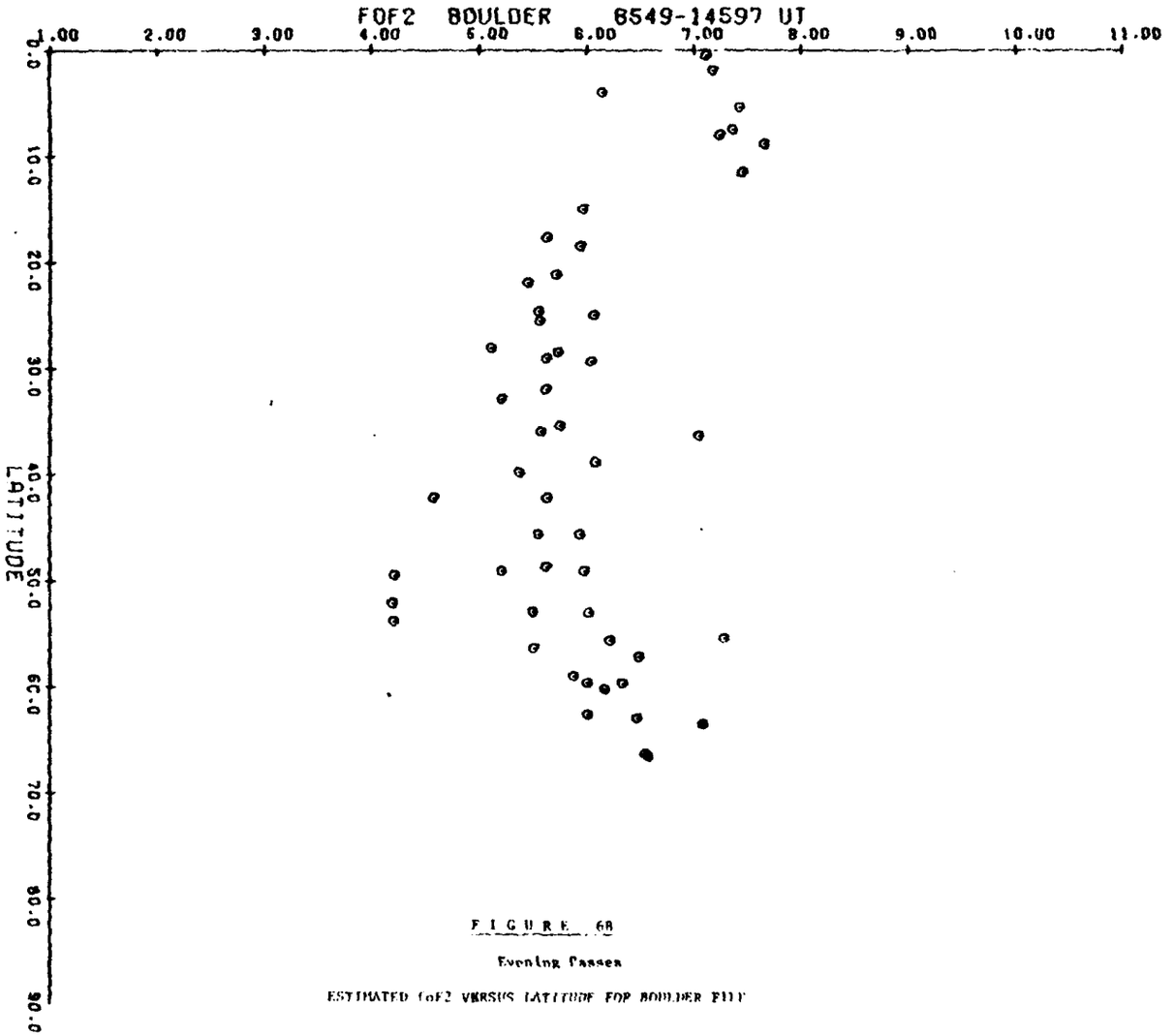

FIGURE 68

Evening Passes

ESTIMATED foF2 VERSUS LATITUDE FOR BOULDER FIT


DA
FILM